Bridging Econometrics and AI: VaR Estimation via Reinforcement Learning and GARCH Models

Fredy Pokou, Jules Sadefo Kamdem, François Benhmad

Bridging Econometrics and AI: VaR Estimation via Reinforcement Learning and GARCH Models

Fredy POKOU [*1], Jules SADEFO KAMDEM [†2], and François BENHMAD [‡3]

[1]Inria, CNRS, Univ. of Lille, Centrale Lille, UMR 9189 - CRIStAL, F-59000 Lille, France
[2,3]MRE UR 209 and Faculty of Economics. Montpellier University, France

April 16, 2025

Abstract

In an environment of increasingly volatile financial markets, the accurate estimation of risk remains a major challenge. Traditional econometric models, such as GARCH and its variants, are based on assumptions that are often too rigid to adapt to the complexity of the current market dynamics. To overcome these limitations, we propose a hybrid framework for Value-at-Risk (VaR) estimation, combining GARCH volatility models with deep reinforcement learning. Our approach incorporates directional market forecasting using the Double Deep Q-Network (DDQN) model, treating the task as an imbalanced classification problem. This architecture enables the dynamic adjustment of risk-level forecasts according to market conditions. Empirical validation on daily Eurostoxx 50 data covering periods of crisis and high volatility shows a significant improvement in the accuracy of VaR estimates, as well as a reduction in the number of breaches and also in capital requirements, while respecting regulatory risk thresholds. The ability of the model to adjust risk levels in real time reinforces its relevance to modern and proactive risk management.

Keywords: Deep reinforcement learning, Directional prediction, Imbalanced class problem, Value-at-Risk

1 Introduction

Forecasting stock prices using empirical data is a central topic in financial research. In recent years, the growth of technology and the massive availability of data have heightened interest in the use of machine learning models in the analysis of financial markets. These models help to capture the inherent complexity of financial data, characterized by its nonlinearity, hidden structures, and dynamic evolution in response to various factors. However, in the context of risk management and portfolio optimization, the analysis of stock market returns is more relevant than the study of asset prices. Returns are often stationary, which makes for a more robust analysis, and, in accordance with the central limit theorem, they can sometimes be approximated by a normal distribution. However, this assumption is questionable given the stylized facts of financial time series: non-linear autocorrelation, asymmetric distribution tails, volatility clustering, and leverage. These features make the prediction of returns more complex than that of prices, as illustrated in figure 1, where we observe that conventional models struggle to predict excess returns, whether positive or negative.

[*]fredypokou@gmx.fr
[†]jules.sadefo-kamdem@umontpellier.fr
[‡]francois.benhmad@umontpellier.fr

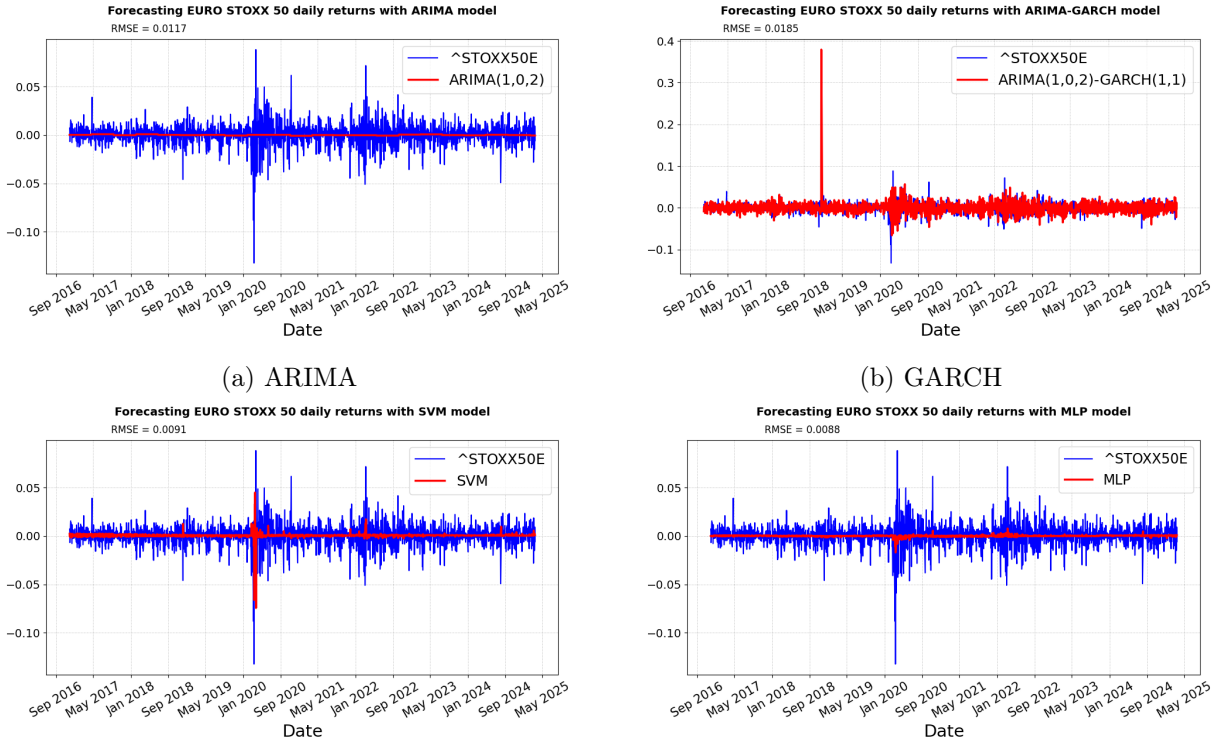

(a) ARIMA (b) GARCH

(c) SVM (d) MLP

Figure 1: Euro Stoxx 50 return forecasts using different models

This difficulty in capturing strong positive and negative variations is also observed in machine learning and deep learning models, despite their great flexibility and ability to model complex non-linear relationships. These models are based on optimization algorithms that require large volumes of data to efficiently learn the underlying dynamics of financial markets, particularly when dealing with rare and extreme events (Pokou, 2022). Extreme events, by definition, are infrequent in financial time series, which limits the capacity of these models to extract exploitable regularities (Fawcett and Provost, 1997). The most machine learning and deep learning models are trained by minimizing mean square error (MSE) or similar loss functions, which give disproportionate weight to errors on the most common values at the expense of extreme events.

These approaches lead to a bias in favor of predictions close to the mean of historical data, reducing the sensitivity of the model to strong market variations (Goodfellow et al., 2016). As a result, even advanced architectures such as recurrent neural networks (RNN), temporal convolutional neural networks (TCN) or hybrid model combinations (e.g. ARIMA-ANN) fail to accurately anticipate these rare events (Zhang, 2003; Tealab, 2018; Pokou et al., 2024b). This difficulty is partly related to the efficient market hypothesis Fama (1970), which postulates that prices incorporate all available information, making their prediction uncertain.

Faced with the difficulty of accurately predicting the returns of the stock market, several authors (Kanas, 2001; Nyberg, 2011; Oh and Sheng, 2011; Alostad and Davulcu, 2017; Becker and Leschinski, 2018; Chandrasekara et al., 2019) have proposed reformulating this problem into a classification task, focusing no longer on the exact value of the returns, but on their sign (positive or negative). This approach, known as directional return prediction, is based on the idea that the key to many investment strategies is not to anticipate the precise return but rather to determine the future direction of the market. For this purpose, a threshold is defined to classify returns into distinct categories: generally, this threshold is set at zero, thus distinguishing positive from negative returns. However, some studies (Chung and Hong, 2007; Linton and Whang, 2007) have proposed more sophisticated thresholds, based, for example, on multiples of the standard deviation or quantiles of the return distribution, to better capture significant market movements.

In this study, we extend this approach by adopting a threshold, inspired by the work of Nevasalmi (2020). Rather than simply distinguishing between positive and negative returns, we introduce a finer classification that isolates some of the noise and better identifies extreme returns, whether strongly positive or negative. This approach refines the prediction by focusing on the most significant market movements. However, it leads to class imbalance, making the classification task more complex. To the best of our knowledge, this problem has been little explored in the context of financial time series. However, financial risk management relies on measures such as Value-at-Risk (VaR), which estimates the maximum potential loss of a portfolio over a given time horizon with a certain level of confidence. Originally developed in the work of Markowitz (1952, 1959), VaR has been widely adopted in banking regulation (Basel I, II, III). But despite its importance, VaR has certain limitations:

- Overestimation of risk, leading to a waste of capital
- Underestimation of risk, increasing exposure to excessive losses.

These limitations have led to the development of alternative measures, such as Expected Shortfall (ES), which is more mathematically robust but whose backtesting methods remain less well established. In this study, we focus on improving VaR prediction by incorporating directional prediction of returns into its estimation. Traditionally, directional return forecasting relies on statistical and supervised machine learning models, such as logistic regression (LR), gradient boosting (GBM), random forests (RF), neural networks (MLP, LSTM, etc.). (Tang et al., 2008). However, these approaches suffer when there is a class imbalance, which is precisely the case in our study. To mitigate this effect, various rebalancing techniques have been developed:

- Resampling methods: oversampling (SMOTE, ADASYN) or undersampling (ENN, Tomek-Links)
- Ensemble methods: boosting, bagging and random forests
- Cost-sensitive learning, which penalizes errors on the minority class.

However, these approaches can induce bias or overfitting. Deep reinforcement learning (DRL) represents a promising alternative, as it directly learns an optimal policy for managing class imbalance. Successfully applied in various fields (Mnih et al., 2013; Gu et al., 2017; Mao et al., 2016; Zhao et al., 2017; Yu et al., 2021), DRL has recently been used in finance (Deng et al., 2016; Liu et al., 2020; Yang et al., 2020; Zhang et al., 2020; Pokou et al., 2024a). Its integration into our approach improves the robustness of directional forecasting and, by extension, VaR estimation. The use of Deep Reinforcement Learning (DRL) to estimate risk measures such as Value-at-Risk (VaR) and Expected Shortfall (ES) has recently attracted growing interest in quantitative finance. Morimura et al. (2012) proposed a parametric approach to estimate the density of returns via an extension of the Bellman equation, leading to robust and risk-sensitive TD learning algorithms. In a similar framework, Ying et al. (2022) developed the CVaR-Proximal-Policy-Optimization (CPPO) algorithm, constraining policy optimization to a bound on Conditional Value-at-Risk (CVaR), thus guaranteeing more robust learning in the face of uncertainties.

Furthermore, Barrera et al. (2022) have studied nonparametric learning of VaR and ES using generalization bounds derived from Vapnik-Chervonenkis statistical theory, highlighting approximation methods based on quantile regressions and neural networks. From a complementary perspective, Clements et al. (2019) have examined epistemic and random uncertainties in DRL applied to Q values, proposing a DQN algorithm adjusted for these uncertainties and demonstrating improved stability of risk estimates. In addition, recent work on robust estimation of ES in heavy-tailed distributions has highlighted the limitations of traditional approaches and the potential contribution of DRL to capture the extreme dynamics of financial returns. These contributions illustrate the advances of DRL in financial risk modeling while raising challenges regarding the interpretability of learned policies and the stability of risk estimates in uncertain environments.

In contrast to this work, our approach applies DRL to directional forecasting of stock returns in order to improve VaR estimation. By reformulating the problem as a directional classification task rather than a classical return regression, we take advantage of DRL to better manage the class imbalance and refine the forecast accuracy. This approach aims to overcome the limitations of traditional methods by providing a more reliable estimate of risk, thus minimizing the overestimation and underestimation errors common in VaR calculations.

The main contribution of this paper lies in the development of a new empirical approach to Value-at-Risk (VaR) estimation. In contrast to traditional approaches, our method takes advantage of directional prediction of returns to dynamically adjust the VaR, enabling better adaptation to market fluctuations. In addition, it incorporates efficient class imbalance management thanks to the capabilities of Deep Reinforcement Learning (DRL), which considerably improves the stability and relevance of risk forecasts. Finally, this approach stands out for its ability to increase the accuracy and robustness of VaR, simultaneously reducing the number of violations and excessive capital allocation, thus offering a more effective framework for financial risk management.

The paper is structured to guide the reader progressively through our methodological approach and its empirical implications. First, Section 2 introduces the methodological framework, detailing the theoretical foundations and models used for adaptive Value-at-Risk estimation. The next sections 3 and 4 present the empirical results obtained, together with an in-depth analysis of their robustness, highlighting the performance of our approach compared to conventional methods. Finally, Section 5 concludes the study by summarizing the main contributions and opening the discussion on prospects for improvement and future application of our model.

2 Methodology

Let P_t be the closing price of an asset at time t, so the logarithmic return at time t over a unit time interval is defined as $r_t = \log(P_t/P_{t-1})$.

2.1 Value-at-Risk

The Value-at-Risk (VaR) is the quantile α of the return distribution and represents the loss that will be exceeded in a proportion $\alpha \times 100\%$ of cases during the next period. Then we have :

$$P(r_{t+1} < -VaR^{\alpha}_{t+1}) = \alpha \tag{1}$$

where $\alpha \in [0, 1]$ is a probability generally set at 0.05 or 0.01. After a short demonstration in a few steps, we have the following :

$$VaR_{t+1}(\alpha) = -F_{r_{t+1}}(\alpha) \tag{2}$$

where $F_{r_{t+1}}(\alpha)$ represents the inverse return distribution function, also known as the quantile function.
VaR has gained popularity due to the simplicity of implementation and the ability to make no assumptions about the parametric form of return distributions. Although we may be tempted by non-parametric solutions, it is important to remember that parametric VaR is very useful.

In particular, a model capable of taking into account stylized facts about asset return distribution was defined. The normal distribution is often used, except that unconditional return distributions usually have much fatter tails. Using first two conditional moments of the distribution, it is possible to present returns time series in this form:

$$r_t = \mu_t + \sigma_t z_t \tag{3}$$

where r_t is the return at time t, μ_t is the conditional mean, σ_t is the conditional volatility of the return and z_t is the residual of the process (innovation term).

It is assumed that z_t are distributed independently and identically and follow a known theoretical distribution with zero mean and unit variance. If the random variable z_t is normally distributed, we have :

$$VaR_{t+1}(\alpha) = -\mu_{t+1} - \sigma_{t+1}\phi^{-1}(\alpha) \tag{4}$$

where ϕ^{-1} is the cumulative distribution function of a standard normal variable.

Given these stylized facts, and in particular the nonnormality of asset return distributions, a standardized Student distribution would be the most plausible (with zero mean and unit variance) with ν degrees of freedom, giving :

$$VaR_{t+1}(\alpha) = -\mu_{t+1} - \sigma_{t+1}t_{\nu}^{-1}(\alpha) \tag{5}$$

where t_ν denotes the distribution function of Student's standard distribution.
This expression will be useful for independently modeling the dynamics of μ_{t+1} and σ_{t+1}. In our case, μ_{t+1} will be modeled as arithmetic mean returns, which take values very close to zero. Conditional volatility σ_{t+1} will be modeled directly using the GARCH (resp. GJR-GARCH) time series.

2.2 GARCH models

Introduced by Bollerslev (1986), the GARCH(p,q) model can be defined by assuming that $\{r_t\}_{t\in\mathbb{Z}}$ is a stochastic process decomposable in terms of expected returns and residuals, as follows:

$$r_t = \mu + \epsilon_t$$

where

$$\begin{cases} \epsilon_t & = \sigma_t z_t \\ \sigma_t^2 & = \alpha_0 + \sum_{i=1}^{p} \alpha_i \epsilon_{t-i}^2 + \sum_{j=1}^{q} \beta_j \sigma_{t-j}^2 \end{cases} \tag{6}$$

with $0 < \alpha_0$, $\forall i = 1, \ldots, p$, $0 < \alpha_1 \leq 1$, $\forall j = 1, \ldots, q$, $0 < \beta_1 \leq 1$ and independent, identically distributed variable z_t.

The GARCH (1,1) model is the simplest and most commonly used univariate model and can be defined as follows

$$\begin{cases} \epsilon_t & = \sigma_t z_t \\ \sigma_t^2 & = \alpha_0 + \alpha_1 \epsilon_{t-1}^2 + \beta_1 \sigma_{t-1}^2 \end{cases} \tag{7}$$

where the variance process σ_t^2 in GARCH(1,1) is stationary when $\alpha_1 + \beta_1 < 1$.
The convergence rate depends on $\alpha_1 + \beta_1$. As persistence is closer to 1, it takes longer for a shock to be forgotten by the market.

Glosten, Jagannathan, and Runkle (1993) proposed the GJR-GARCH(p,q) model to overcome GARCH's inability to differentiate between negative and positive shocks and to take leverage into account. It can be defined as follows:

$$\begin{cases} \epsilon_t & = \sigma_t z_t \\ \sigma_t^2 & = \alpha_0 + \sum_{i=1}^{p} (\alpha_i + \gamma_i \mathbb{1}_{\epsilon_{t-i}<0}) \times \epsilon_{t-i}^2 + \sum_{j=1}^{q} \beta_j \sigma_{t-j}^2 \end{cases} \tag{8}$$

In particular, GJR-GARCH(1,1) is expressed as follows:

$$\begin{cases} \epsilon_t & = \sigma_t z_t \\ \sigma_t^2 & = \alpha_0 + (\alpha_1 + \gamma \mathbb{1}_{\epsilon_{t-1}<0}) \times \epsilon_{t-1}^2 + \beta_1 \sigma_{t-1}^2 \end{cases} \tag{9}$$

where positivity of conditional variances is ensured by $\alpha_0 > 0$, $\alpha_1 \geq 0$, $\beta_1 \geq 0$ and $\alpha_1 + \gamma \geq 0$, therefore, if $\gamma > 0$, bad news has a greater impact on conditional variance than good news, and in addition, stationarity of variances is possible provided that $\alpha_1 + \beta_1 + 0.5\gamma < 1$.

2.3 Threshold selection for directional prediction

Although regression models were the most intuitive approach to predicting future values of stock market asset returns, the current trend shows that classification models appear to have better predictive power. Except that this requires transforming a prediction problem into a classification problem. Classes are determined according to the desired goal via a threshold. In trading, for example, it is possible to construct strategies based on return signs (positive or negative) or excess returns, i.e. the difference between returns and the risk-free rate (r_f). In directional prediction, binary dependent variables are created from return series using an indicator function

$$y_t(c) = \mathbb{1}_{\{r_t > c\}} \quad \text{or} \quad y_t(c) = \mathbb{1}_{\{r_t - r_f > c\}}$$

where c is a given threshold (often $c = 0$).

In our study, given that the objective is to improve value-at-risk performance, the chosen threshold is the lowest VaR violation.

$$\begin{aligned} c &= \max\{r_{k+1} < VaR_{k+1}(\alpha)\}_{k \in \{1,\dots,H\}} \\ y_t(c) &= \mathbb{1}_{\{r_t \leq c\}} \end{aligned} \tag{10}$$

H is the number of VaR violations.

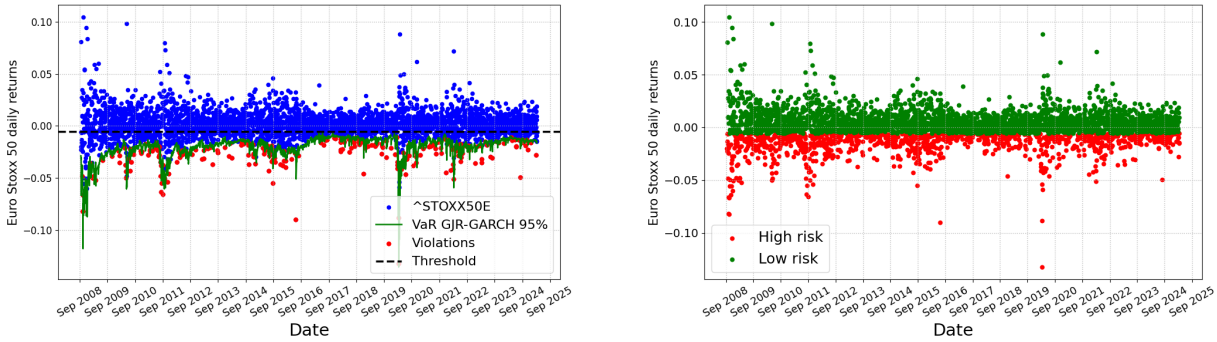

(a) Threshold selection

(b) The two return classes

Figure 2: Illustration characterization of threshold and return classes

Figure 2a illustrates our threshold choice. It allows us to create two classes representing low-risk ($y_t(c) = 0$) and high-risk ($y_t(c) = 1$) returns, respectively, as shown in figure 2b.

2.4 Proposed VaR model

Let $VaR_{t+1}(\alpha)$ be the value-at-risk with a threshold α calculated using a GARCH or GJR-GARCH model. Let us consider a classification model that assigns at each time t+1 a predicted risk category among two possible states:

- "Low risk": low level of risk
- "High risk": high level of risk

Definition 1 (Classification-Adjusted Value at Risk)**.** *The Classification-Adjusted Value at Risk, noted $VaR_{ML}(\alpha)$ is defined as follows:*

$$VaR_{ML}(\alpha) = \begin{cases} (1 - b_1) \cdot VaR_{t+1}(\alpha), & si\ \hat{r}_{t+1} = \text{"Low risk"} \\ (1 + b_2) \cdot VaR_{t+1}(\alpha), & si\ \hat{r}_{t+1} = \text{"High risk"} \end{cases} \tag{11}$$

where :

- $b_1, b_2 \in \mathbb{R}^+$ *are calibration parameters determining the extent of the reduction or increase in* $VaR_{t+1}(\alpha)$.
- $\hat{r}_{t+1}$ *is the prediction of the future risk level made by the machine learning models we will present in the next section.*

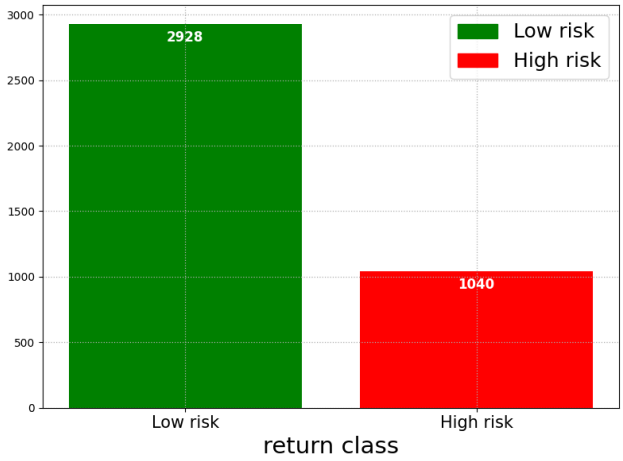

Figure 3: Proportion of different return classes

The proposed VaR model has properties identical to those of the original VaR. Knowing that it is not possible for $\hat{r}_{t+1}$ to have two risk levels at the same time, one of equation (11)'s components becomes null, and with VaR's positive homogeneity property, the proof is obvious.

2.5 Machine Learning

In figure 3, we can see that we are dealing with an unbalanced class problem. This is a major challenge in training traditional Machine Learning models, including logistic regression (Dreiseitl and Ohno-Machado, 2002), Support Vector Machine (SVM) (Vapnik, 1999; Tang et al., 2008) and various neural network architectures such as perceptron (ANN), multilayer perceptron (MLP) (Rosenblatt, 1958; Murtagh, 1991), recurrent neural networks (RNN) (Ampomah et al., 2020; Sunny et al., 2020) and Temporal Convolutional Network (TCN) (Lea et al., 2016).

In such scenarios, models tend to favor the majority class, leading to a strong imbalance in predictions, where minority cases are often ignored. Although sampling techniques such as under-sampling (ENN[1], Random Undersampling, Tomek Links) (Kotsiantis et al., 2006; Barandela et al., 2004; Elhassan and Aljurf, 2016; Zeng et al., 2016; Pereira et al., 2020) and over-sampling (ADASYN[2], SMOTE[3], Random Oversampling) (Chawla et al., 2002; Han et al., 2005; Zhang and Li, 2014) have been developed to alleviate this problem, they themselves present certain limitations.

Undersampling reduces the size of the majority class, which can lead to a loss of valuable information and impair overall model performance. In contrast, oversampling artificially increases the size of the minority class, but at the cost of an increased risk of overfitting, as synthetic observations may not faithfully reflect the actual distribution of the data. Another key challenge in these contexts lies in error measurement and model optimization. Standard cost functions such as cross-entropy loss or mean square error (MSE) are often inadequate for unbalanced classes, as they are dominated by the majority class.

This results in weight updates that minimize overall loss, but without improving the model's ability to detect the minority class. Even by adjusting the weights of the loss function or modifying the evaluation metrics (such as using F1-score or recall instead of simple accuracy), classical supervised models struggle to learn effective representations in such an environment. Given these limitations, the Double Deep Q-Network (DDQN) appears to be a promising alternative. Unlike purely supervised models, DDQN is based on reinforcement learning, where the agent learns to optimize its decisions by interacting with a dynamic environment.

[1] Edited Nearest Neighbors
[2] Adaptive Synthetic Sampling
[3] Synthetic Minority Over-sampling Technique

This approach enables more efficient exploration of classification strategies and better adaptation to imbalances, without depending directly on a pre-established class distribution. By maximizing a reward function, DDQN learns to handle rare classes in a more robust and adaptive way, offering a better alternative to classical supervised learning methods.

2.6 Reinforcement learning

Supervised learning, to which the above-mentioned models belong, relies on the use of labeled data to establish a relationship between inputs (features) and outputs (labels). The aim is to learn a function that, after training, can generalize to new data and correctly predict the corresponding class. This type of learning is effective when the data are well balanced and when the relationship between the explanatory variables and the target variable is sufficiently clear. However, it has significant limitations when applied to complex and dynamic problems, such as those involving high-class imbalance or requiring sequential decision-making.

In contrast, reinforcement learning proposes a fundamentally different paradigm. Rather than optimizing a cost function by minimizing the error between predictions and actual labels, the goal is to learn an optimal policy that maximizes the cumulative reward obtained by an agent interacting with an environment. This process is based on a trial-and-error loop, where the agent explores different actions, observes their consequences, and gradually adjusts its strategy according to the rewards received. This approach enables models to learn adaptively and autonomously, which is particularly useful for problems where the underlying rules are dynamic or partially unknown.

Introduced by Sutton and Barto (1998), reinforcement learning was designed to overcome the limitations of dynamic programming approaches (Puterman, 2014) and Monte Carlo methods (Gilks et al., 1995). Unlike dynamic programming, which requires explicit knowledge of the environment model and quickly becomes inapplicable in large state spaces, and Monte Carlo methods, which cannot easily exploit the temporal structure of decisions, reinforcement learning allows for a more flexible and scalable approach to the sequential decision problem.

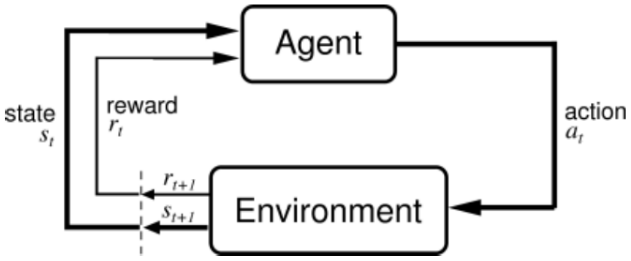

Figure 4: Agent-environment interaction model (Sutton and Barto, 1998)

The agent-environment interaction model is illustrated in figure 4. This problem is based on the Markov Decision Process (MDP) (White III and White, 1989), which formalizes the interaction between an agent and its environment in terms of states, actions, rewards, and probabilistic transitions. One of the key concepts of this approach is the value function, which estimates the expected future reward for a given action in a specific state. The optimization of this function is based on the Bellman equation, which describes the recursive relationship between state values and future rewards, and forms the basis of many modern reinforcement learning methods, including deep neural network approaches such as the Double Deep Q-Network (DDQN). Thus, by exploiting the principles of reinforcement learning and MDP, models based on autonomous agents can learn to make optimal decisions in complex and uncertain environments, where classical supervised approaches encounter significant limitations. This ability to adapt and learn progressively makes reinforcement learning a particularly relevant alternative in contexts where data are unbalanced, interaction rules evolve, and decision making needs to be optimized over the long term.

2.6.1 Markov Decision Process

A Markov decision process is a 5-tuple $\langle \mathcal{S}, \mathbb{A}, \mathcal{P}, \mathcal{R}, \gamma \rangle$ where :

- $\mathcal{S}$ is a finite set of states that the environment can reach such that they satisfy Markov's property.
- $\mathbb{A}$ is a finite set of actions (action space). For our classification problem, $a \in \mathbb{A} := \{0, 1\}$ where 0 represents the majority class (low risk) and 1 represents minority class (high risk). The action a taken by an agent consists of predicting a class label.
- $\mathcal{P}$ is a state transition function.
  We have : $\mathcal{P} : \mathcal{S} \times \mathbb{A} \times \mathcal{S} \to [0, 1]$.
  For a MDP, next state and reward depend solely on the current state and action. The probability of going from state s to state s' at time t by performing action a is :

$$P(s', a, s) = \mathbb{P}[s_{t+1} = s' | s_t = s, a_t = a]$$

- $\mathcal{R}$ gives a signal on actions quality performed by the agent during its learning phase. The reward function can be defined as the expected value of the reward of the action a' when moving from one state s to the next s'.

$$R(s', a, s) = \mathbb{E}[r_{t+1} | s_t = s, a_t = a, s_{t+1} = s']$$

  The agent is rewarded positively if it correctly classifies a sample (true positive and true negative), otherwise it is rewarded negatively (false positive and false negative). The reward r_t can be defined as :

$$R_t = \begin{cases} +\rho & a_t \text{ is True Negative} \\ -\rho & a_t \text{ is False Negative} \\ +1 & a_t \text{ is True Positive} \\ -1 & a_t \text{ is False Positive} \end{cases}$$

  where $\rho \in]0, 1]$ more precisely equals the ratio of minority class cardinal to majority class cardinal.

  1. True Negative (TN):
     The model predicts "Low risk" and the observation is actually "Low risk". In this case, the prediction is correct. The reward function awards $+\rho$ to encourage the agent to correctly classify the majority class, without penalizing it too much.
  2. False Negative (FN):
     The model predicts "Low risk", but the observation is actually "High risk". This is a critical error, as a high-risk individual has been classified as "Low risk". This error is often more serious than the others The reward function assigns a penalty of $-\rho$, which is consistent with the weighting of the classes, since the minority class is less frequent and deserves more attention.
  3. True Positive (TP):
     The model predicts "High risk" and the observation is actually "High risk". This is a good prediction and should be encouraged. The associated reward is $+1$, which correctly rewards the detection of critical cases.
  4. False Positive (FP):
     The model predicts "High risk", but the observation is actually "Low risk". This is an error where a "Low risk" individual is classified as "High risk". Although this error is less serious than a FN, it has a cost in terms of unnecessary processing of a false alarm signal. The reward function assigns a penalty of -1 to limit false positives.

- γ ($\gamma \in [0, 1]$)is a discount factor used to balance immediate and future reward.

2.6.2 Policy

A policy $\pi : \mathcal{S} \rightarrow \mathbb{A}$ defines the agent's behavior at time t where π_t denotes the action a performed by the agent in state s :

$$\pi_t(a|s) = \mathbb{P}(a_t = a|s_t = s) \tag{12}$$

The policy π can be considered as a classifier and the agent must be able to learn to perform actions to maximize the expected total discounted return G_t, according to the following equation.

$$G_t = \sum_{k=0}^{\infty} \gamma^k R_{t+k+1} \tag{13}$$

where $\gamma \in [0.1]$ is the discount rate.
The optimal policy π^* to obtain the expected maximum return from all states

$$\pi^* = arg \max_{\pi} \mathbb{E}[G_t|\pi] \tag{14}$$

2.6.3 State-Value function

The state value function is the expected return on a given state s, which then follows a policy π (Szepesvári (2010)), that is,

$$\upsilon_\pi(s) = \mathbb{E}_\pi[G_t|s_t = s] \tag{15}$$

Thus, the optimal state value function is obtained under the optimal policy π^* as:

$$\upsilon^* = \max_{\pi} \upsilon_\pi(s) \ , \forall s \in \mathcal{S} \tag{16}$$

2.6.4 Action-value function

The Q function, or the action value of the function, is the expected return from the state s, by taking action a, then by following policy π, i.e.,

$$Q_\pi(s, a) = \mathbb{E}_\pi[G_t|s_t = s, a_t = a] \tag{17}$$

The optimal Q-function is the maximum of all policies:

$$Q^*(s, a) = \max_{\pi} Q_\pi(s, a) \quad \forall s \in \mathcal{S}, \ a \in \mathbb{A} \tag{18}$$

According to Bellman's expectation equation (Dixit (1990)), the Q function can be expressed as follows :

$$Q_\pi(s, a) = \mathbb{E}_\pi[R_t + \gamma Q_\pi(s_{t+1}, a_{t+1})|s_t = s, a_t = a] \tag{19}$$

The optimal policy is found by maximizing the optimal state value function $Q^*(s, a)$ presented in equation (18). In other words, the best policy can be found by greedily choosing action in each state, which can be defined as :

$$\pi^*(a|s) = \begin{cases} 1 & \text{if } a = arg \max_{a} Q^*(s, a) \\ 0 & \text{else.} \end{cases} \tag{20}$$

Using Bellman's optimality equation, we get :

$$Q^*(s, a) = \mathbb{E}_\pi[R_t + \gamma \max_{\pi} Q_\pi(s_{t+1}, a_{t+1})|s_t = s, a_t = a] \tag{21}$$

2.6.5 Q-Learning

Since finding an optimal policy meant maximizing the Q function, Sutton (1988) proposed the temporal difference (TD) learning algorithm, which belongs to the class of tabular algorithms. It is based on a bootstrapping operation that uses estimated values of future states to update the estimate of current state. Then it saves the sample in a Q-table, from which the new estimate is obtained from a sample of possible options for the next state.

However, it becomes impossible to perform this backup due to enormous table size when environment has a large number of states or a continuous state space. In this sense, Watkins (1989) introduced one of the most popular algorithms, Q-learning, which is an extension of the temporal difference to overcome this limitation. So, instead of directly estimating a state value, we estimate each state-action pair value.

The goal is to gradually learn to associate states with actions in order to maximize expected rewards. These expected rewards (Q-values) are stored in a lookup table (Q-table), which functions as a memory that is updated as the agent explores its environment. The update rule is as follows:

$$Q_\pi(s_t, a_t) \leftarrow (1-\alpha)Q_\pi(s_t, a_t) + \alpha\left(R_{t+1} + \gamma \max_{a_{t+1}\in\mathbb{A}} Q_\pi(s_{t+1}, a_{t+1})\right) \tag{22}$$

where

- $Q_\pi(s_t, a_t)$ is the Q-value for state s_t and action a_t.
- α is the learning rate that controls the size of the update.
- R_{t+1} is the reward obtained after taking action a_t in state s_t.
- γ is the discount factor.
- $\max_{a_{t+1}\in\mathbb{A}} Q_\pi(s_{t+1}, a_{t+1})$ is the best Q-value for the next state.

2.6.6 Deep Q-Network

In Q-learning, the agent must maintain and update a set of Q-values for all pairs of states and actions. However, in some applications, billions of unique possible states and several available actions are required. As a result, the time and cost of calculating and updating all Q-values become virtually unfeasible, which is known as "the curse of dimensionality". Deep Q Network (DQN) solves this problem by using a deep neural network to approximate the Q-function.

We then have $Q^*_\pi(s_t, a_t) \approx Q_\pi(s_t, a_t, \theta)$ where θ is a vector containing all weights and biases of the neural network. This neural network takes as input the current state s_t and the action a_t and estimates the Q-value. Furthermore, as mentioned earlier, DQN introduces Experience Replay and target network $\hat{Q}_\pi$, two important enhancements that stabilize learning. $\hat{Q}_\pi$-network used to estimate the target value is then :

$$y_t^{DQN} = R_{t+1} + \gamma \max_{a_{t+1}\in\mathbb{A}} \hat{Q}_\pi(s_{t+1}, a_{t+1}; \theta^-) \tag{23}$$

where θ are the weights of the target network.
After randomly sampling mini-batches of experiments from the replay buffer, these experiments are used to train the Q-network to minimize the difference between predicted and target Q-values. The weights of the neural network (θ^-) are updated by the gradient descent of the loss function, which is represented by the following formula.

$$\mathcal{L}(\theta) = \mathbb{E}\left[\left(y_t^{DQN} - Q_\pi(s_t, s, a_t; \theta)\right)^2\right] \tag{24}$$

where θ are the weights of the current network.

To avoid instability during learning, Q-network ($Q_\pi(s, a; \theta)$) is updated at each learning step, whereas the target network ($Q_\pi(s, a; \theta^-)$) is updated less regularly by copying weights from Q-network.

2.6.7 Double Deep Q-Network

During Q-value estimation for each possible action in a given state with Deep Q-Network (DQN), a frequent problem is overestimation can lead to suboptimal policy selection. This is because the DQN uses the same network to guide exploration (maximum action selection) and to evaluate this action. Van Hasselt et al. (2016) proposed double deep Q-network (DDQN). An algorithm that advocates using two separate networks to estimate and evaluate actions, thus reducing over-estimation and improving learning stability. Instead of using update function expressed by equation (22), DDQN strategy is based on update functions presented in Jang et al. (2019)'s paper :

$$Q_{\pi}^{(1)}(s_t, a_t) \leftarrow (1-\alpha)Q_{\pi}^{(1)}(s_t, a_t) + \alpha \left[R_{t+1} + \gamma \max_{a_{t+1} \in \mathbb{A}} Q_{\pi}^{(2)}(s_{t+1}, a_{t+1}) \right] \tag{25}$$

$$Q_{\pi}^{(2)}(s_t, a_t) \leftarrow (1-\alpha)Q_{\pi}^{(2)}(s_t, a_t) + \alpha \left[R_{t+1} + \gamma \max_{a_{t+1} \in \mathbb{A}} Q_{\pi}^{(1)}(s_{t+1}, a_{t+1}) \right] \tag{26}$$

Q-function ($Q_{\pi}^{(1)}$) changes its value according to the value of the other Q-function ($Q_{\pi}^{(2)}$), and both functions determine the action. Dans ce cas, la valeur cible du DQN peut alors être écrite comme suit :

$$y_t^{DDQN} = R_{t+1} + \gamma \max_{a_{t+1} \in \mathbb{A}} \hat{Q}_{\pi} \left(s_{t+1}, arg \max_{a_{t+1} \in \mathbb{A}} Q_{\pi}(s_{t+1}, a_{t+1}; \theta); \theta^{-} \right) \tag{27}$$

Consequently, the Q-network selects the action a_t that results in the maximum Q-value for the next state, and the target network calculates the estimate of the Q-value based on the action selected previously. As with DQN, the use of the replay buffer makes learning more stable and efficient. During the learning process, experience replay is used to update the main network parameters, minimizing a differentiable loss function which, in the DDQN case, has the following form:

$$\mathcal{L}^{DDQN}(\theta) = \mathbb{E}\left[\left(y_t^{DDQN} - Q_{\pi}(s_t, a_t; \theta) \right)^2 \right] \tag{28}$$

It also updates the second network weights θ, which are replaced by the target network weights θ^{-}. The weights of both networks are updated at different times, rather than simultaneously. At each learning stage, the valuation network is used to select the optimal action, but the target network is used to evaluate this action. Periodically, weights from the evaluation network are copied to the target network.

3 Empirical results

In this paper, we evaluate the performance of the proposed Value-at-Risk (VaR) model on the Euro Stoxx 50 index, a benchmark index of the 50 largest market capitalizations in the Eurozone. The data used come from Yahoo[4] Finance datastream, covering the period from September 1, 2008 to March 13, 2025. The levels of risk of high risk and low risk will be defined according to the methodology presented in Section 2.3 and shown in figure 2b. An intuitive approach to predicting future risk levels would be to use the lagged returns of the individual components of the Euro Stoxx 50.

However, this methodology has several major limitations. Since its inception, the Euro Stoxx 50 has undergone several periodic revisions, with companies added or removed to reflect developments in European financial markets. This dynamic leads to discontinuity in the data series, which would complicate the training of machine learning models. This is because models based on these components would require constant updates whenever the index changed, making the analysis less robust and difficult to generalize. To overcome these limitations and ensure a more robust, generalizable, and stable approach over time, we opted for a more relevant selection of explanatory variables. As a first step, the stock market indices of the main economies in the euro zone would allow us to capture the overall economic development of European countries and identify general market trends.

[4] https://fr.finance.yahoo.com/

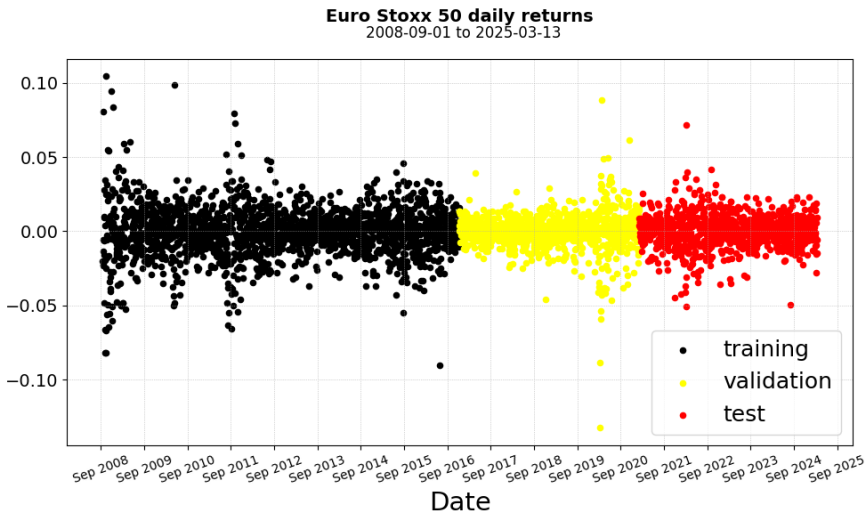

Figure 5: Data set splitting

Then, the currencies influencing European financial markets, which play a key role in the competitiveness of exporting companies and the attractiveness of foreign investment in Europe. We consider strategic currency pairs such as EUR/USD and EUR/GBP . In addition to macroeconomic variables, certain technical indicators are integrated to detect trends and signals of market reversal. To ensure a reliable and rigorous evaluation of the model, we divided the data chronologically into three distinct samples, as shown in figure 5. The training sample, which will make up the bulk of the data, is used to train the model by learning the relationships between the explanatory variables and the target variable. The validation set will be used to adjust the model's hyperparameters and prevent overfitting, thus guaranteeing a better generalization. Then there is the test sample, which will be used only after training and validation, to assess the model's actual performance on new observations and measure its ability to make reliable predictions in an unknown environment.

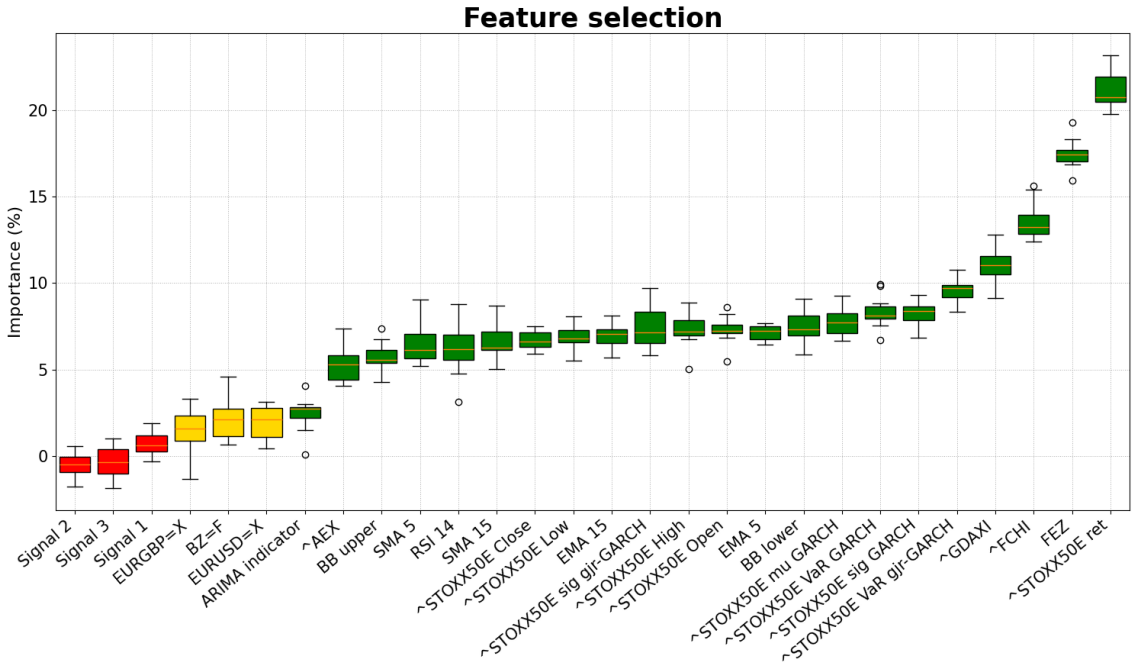

Figure 6: Features selection

The variables were selected using the Boruta algorithm, a robust method specially designed for machine learning models. This algorithm determines the most relevant variables for predicting the risk level of financial asset returns, by identifying variables with a significant influence.

The Boruta algorithm (Kursa and Rudnicki, 2010; Kursa et al., 2010) is particularly well suited to complex datasets, such as those encountered in the financial field, where relationships between variables are often nonlinear and difficult to model. Analysis of the importance of variables using the Boruta algorithm (see figure 6) reveals a clear hierarchy of risk factors. It is interesting to note that the past return of the Eurostoxx 50 at time $t-1$ (^STOXX50E ret) only explains around 20% of the prediction, which may seem relatively modest given its direct link with the level of risk.

This limited contribution can be interpreted by the fact that market dynamics rapidly integrate past information, making simple returns less informative in non-linear models where memory effects, conditional volatility and structural interdependence predominate. For comparison, FEZ, an ETF that faithfully replicates the Eurostoxx 50, provides additional information (17%) that could capture intraday price adjustments, liquidity effects, or market expectations not contained in the raw index. CAC 40 (^FCHI), representing a major component of Eurostoxx 50, provides an explanation of the order of 13%, reinforcing the idea that sector diversification within the index plays a differentiated role in risk formation.

And, volatility forecasts using the GARCH and GJR-GARCH models (varying significantly between 8 and 10%) confirm that the dynamics of expected volatility are a robust but not exclusive determinant of future risk, suggesting that market-perceived risk incorporates both feedback, structural, and behavioral expectation factors. The low explanatory power of currencies such as EUR/USD (EURUSD=X) or EUR/GBP (EURGBP=X) in predicting risk levels can be explained by their global macroeconomic role, often uncorrelated with the specific dynamics of European equity markets. These currency pairs mainly reflect broad monetary and geopolitical movements whose impact on the risk of the stock index is indirect or delayed.

Similarly, technical trading indicators such as buy/sell signals or ARIMA outputs are often built on local heuristics, and only partially capture structural risk components such as implied volatility, inter-market correlation, or sector sensitivity. Their simplifying and short-termist nature therefore limits their ability to explain complex risk phenomena. Table B1 shows the variables selected based on this algorithm.

Assets	Mean (%)	Std (%)	Skewness	Kurtosis	Min	Max	ADF	Jarque-Bera
EURUSD=X	-0.007	0.724	0.782	113.692	-0.143	0.160	-12.606	2136941.801
EURGBP=X	0.001	0.598	0.166	62.569	-0.111	0.110	-33.930	647122.057
BZ=F	-0.006	2.440	-0.606	13.962	-0.280	0.212	-63.680	32465.986
FEZ	0.019	1.741	-0.409	9.130	-0.133	0.162	-11.813	13887.933
^FCHI	0.017	1.409	-0.188	8.671	-0.131	0.106	-21.735	12451.577
^GDAXI	0.034	1.399	-0.087	8.742	-0.131	0.116	-20.348	12637.285
^AEX	0.022	1.311	-0.327	9.672	-0.114	0.100	-12.401	15532.029
^STOXX50E	0.014	1.429	-0.245	7.909	-0.132	0.104	-21.293	10379.093

Table 1: Descriptive statistics for returns

Features	Mean	Std	Min	Max
^STOXX50E Close	3346.722	706.846	1809.980	5540.690
^STOXX50E High	3370.447	705.616	1823.250	5568.190
^STOXX50E Low	3321.543	707.570	1765.490	5506.570
^STOXX50E Open	3346.747	706.032	1812.780	5531.530
BB upper	3469.825	694.591	2139.143	5597.252
BB lower	3213.444	701.508	1670.766	5324.596
EMA 5	3345.631	703.870	1854.835	5495.911
EMA 15	3342.931	696.996	1954.528	5455.968
SMA 5	3345.639	704.382	1857.532	5490.536
SMA 15	3342.891	698.354	1925.779	5481.875
RSI 14	52.626	11.333	10.728	79.894
^STOXX50E μ GARCH	-0.000	0.002	-0.049	0.024
^STOXX50E sig GARCH	0.013	0.006	0.005	0.057
^STOXX50E sig gjr-GARCH	0.013	0.006	0.005	0.057
^STOXX50E VaR GARCH	-0.021	0.011	-0.138	-0.006
^STOXX50E VaR gjr-GARCH	-0.021	0.011	-0.138	-0.006

Table 2: Descriptive statistics for features

Strategy	Sell	Stay	Buy
Signal 1	3681	143	143
Signal 2	3631	168	168
Signal 3	3662	165	140

Table 3: Descriptive statistics for positions in different trading strategies

Variables	Low risk	High risk
ARIMA indicator	2951	1016
risk level	**2928**	**1039**

Table 4: Descriptive statistics of qualitative variables

The risk levels associated with the returns of the assets at time t have been predicted based on the information available at time $t-1$. This data set includes both quantitative and qualitative variables, which justifies the separate presentation of descriptive statistics in tables 1, 2, 3, and 4, each focusing on a specific category of variables. Table 1 presents the standard descriptive statistics for the time series of returns used in this study. These include the mean, standard deviation, skewness, kurtosis, as well as the results of the Augmented Dickey-Fuller (ADF) test and the Jarque-Bera test.

The ADF test is used to assess the stationarity of the time series, a necessary condition for the appropriate application of econometric models. The results suggest that most of the series, notably the Eurostoxx 50, exhibit stationarity. This finding is further supported by a visual inspection of the data in figure 2, where the return series are seen to fluctuate around a constant mean, which is a key characteristic of stationary behavior. In addition, the Jarque-Bera test systematically rejects the hypothesis of normality for the return distributions. These distributions exhibit significant skewness (positive or negative) and excess kurtosis (greater than 3), indicating the presence of fat tails compared to the normal distribution.

This statistical behavior reflects the non-Gaussian nature of financial return distributions and highlights the presence of extreme events and asymmetries. Given these empirical characteristics, nonnormality, skewness, leptokurtosis, and stationarity, the use of nonlinear models is well justified, as they are better suited to capture the complexity and irregularities present in financial market dynamics. The analysis of the descriptive statistics in table 2 highlights significant scale disparities between the various variables used in the study. Such heterogeneity makes data normalization a crucial preprocessing step, especially within the framework of our hybrid modeling approach that combines GARCH models with machine learning algorithms.

Normalization not only serves to align the scales and mitigate the impact of outliers, but also enhances algorithm performance and convergence. Among the available scaling techniques, Min-Max scaling was selected because of its straightforward implementation and ability to map values linearly within a defined range. Furthermore, tables 3 and 4 provide essential qualitative insights into market conditions.

Table 3 highlights the signals produced by three technical trading strategies: Simple Moving Average Cross (Signal 1), Exponential Moving Average Cross (Signal 2), and Relative Strength Index (RSI, Signal 3). Each of these strategies translates price dynamics into actionable recommendations by classifying market positions as "Buy", "Sell", or "Stay". These positions reflect the prevailing market trend and can serve as a valuable input in decision making for investors or algorithmic trading systems. As such, these trading signals offer a complementary layer of information that enhances the predictive power of our models, particularly in adaptive strategies under uncertain market conditions. Finally, the prediction of risk levels obtained from the ARIMA and ARIMA-ANN models (table 4) offers an additional layer of market insight. These models help forecast future market volatility by identifying high- and low-risk periods, providing essential explanatory variables for subsequent classification models.

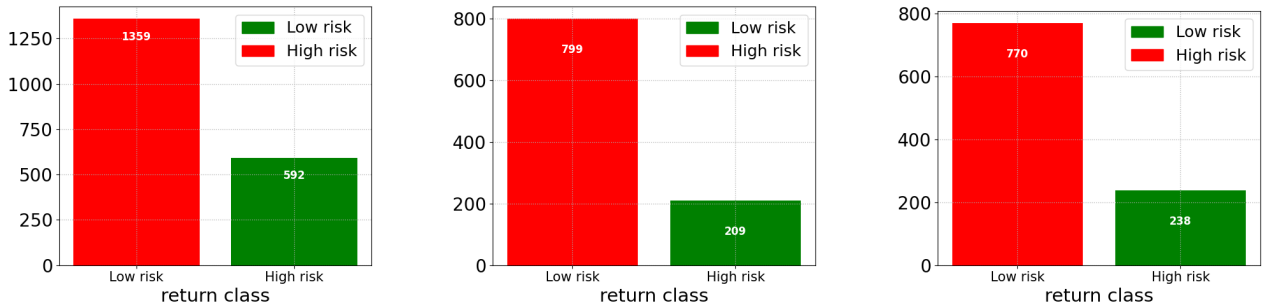

(a) Over training period (b) Over validation period (c) Over testing period

Figure 7: Barplot of different risk levels

Figures 7a, 7b, and 7c show the distribution of observations between the two risk classes on the different samples. In the training sample, for example, there is a clear predominance of the low-risk class, which represents approximately 69.66% of the data, compared to only 30.34% for the high-risk class. This distribution remains relatively similar in the validation and test samples. Although this distribution is asymmetrical, it does not constitute an extreme imbalance. However, this imbalance remains non-negligible in the context of machine learning, as the majority of classification algorithms implicitly assume a balanced distribution between classes.

This misalignment can significantly impair model performance, particularly when it comes to predicting the minority class, which is often the most critical to identify in real-life applications. In our case, the minority class corresponds to high-risk situations, whose detection is of great importance for risk management. Misclassification of this class generates much higher costs than for the majority class. It is therefore essential to adopt appropriate strategies to correct for this increased sensitivity to prediction error. Among existing solutions, data resampling techniques can restore a certain balance between classes. The subsampling approach, which consists in reducing the number of observations in the majority class, proved unsatisfactory in our study, as it generates a significant loss of information and introduces bias in model learning.

In contrast, oversampling methods, in particular the ADASYN (Adaptive Synthetic Sampling) algorithm, have substantially improved performance. By generating new synthetic observations of the minority class, ADASYN enhances the ability of the model to better learn the characteristics of this class while limiting the bias in favor of the dominant class. Although this method implies a longer training time, the trade-off is beneficial for better detection of high-risk cases.

In addition to the Double Deep Q-Network (DDQN), which belongs to the family of deep reinforcement learning algorithms, our study also employs supervised learning techniques such as the Multi-Layer Perceptron (MLP) and the Temporal Convolutional Network (TCN). To address the issue of class imbalance in the dataset, all other supervised learning models are systematically combined with the ADASYN (Adaptive Synthetic Sampling) oversampling technique. This includes traditional models such as Logistic Regression (LR), Support Vector Machines (SVM), and basic neural network architectures such as the Single-Layer Perceptron (ANN).

Another challenge associated with imbalanced classification problems is the selection of appropriate evaluation metrics. Relying solely on accuracy can be misleading: a high accuracy score may simply reflect the model's tendency to predict the majority class, completely overlooking its ability to identify minority class instances. This is particularly problematic when the minority class carries higher misclassification costs, as is often the case in financial risk prediction. To provide a more reliable and comprehensive evaluation of model performance, we incorporate a set of complementary metrics: the F1-score, which balances precision and recall; recall, which assesses the model's ability to detect actual positive cases; precision, which measures how many of the predicted positives are true; and the geometric mean (G-mean), which captures the balance between classification performance on both classes.

These metrics offer a more nuanced understanding of the classifiers' capabilities, especially in skewed class distributions like those in our dataset.

Metric	LR	SVM	ANN	MLP	TCN	RL
Accuracy	0.616	0.639	0.618	0.719	0.788	0.835
F1-score	0.375	0.370	0.368	0.499	0.587	0.668
Recall	0.283	0.290	0.280	0.396	0.492	0.574
Precision	0.555	0.512	0.536	0.675	0.727	0.799
G-Mean	0.489	0.494	0.485	0.596	0.672	0.735

(a) On validation sample

Metric	LR	SVM	ANN	MLP	TCN	RL
Accuracy	0.514	0.524	0.530	0.678	0.720	0.794
F1-score	0.412	0.431	0.398	0.527	0.595	0.661
Recall	0.289	0.300	0.285	0.403	0.452	0.540
Precision	0.723	0.765	0.660	0.761	0.870	0.853
G-Mean	0.492	0.508	0.485	0.602	0.653	0.714

(b) On testing sample

Table 5: Model performance

The comparative analysis of the classification models presented in table 5 highlights the outstanding performance of the Temporal Convolutional Network (TCN) and Deep Reinforcement Learning (RL) models, particularly in validation and test samples. Of all the models evaluated, RL stood out as the best performer in all indicators, with an accuracy of 83.5% in validation and 79.4% in test, as well as the best F1-score (0.668 in validation, 0.661 in test). The TCN model also performed well, with an accuracy of 78.8% in validation and 72% in test, just behind the RL model.

In addition, the Recall and G-Mean scores confirm the RL's robustness, particularly its ability to detect the minority class, which is generally more difficult to classify in unbalanced problems. The RL achieves a Recall of 0.574 in validation and 0.54 in test, the highest values of all the models, which is crucial in a context where misclassification of the high-risk class entails significant costs. The G-Mean, a synthetic indicator that combines precision and recall, corroborates this finding, with 0.735 (validation) and 0.714 (test), reflecting a good balance in the performance of the two classes.

The superiority of RL over TCN and MLP can be explained by the very nature of deep reinforcement learning, which relies on the dynamics of interaction with the environment to enable optimized sequential decision making. Unlike supervised methods such as MLP or TCN, RL learns to maximize a reward function through optimal policies, giving it a strategic advantage in contexts where decisions must take into account time dependency and the future impact of a current prediction. This adaptive capacity, reinforced by mechanisms such as exploration/exploitation and Q-value discounting, enables RL to better manage the uncertainty and temporal structure of financial data.

In short, the key metrics to highlight in this analysis are F1-score, Recall and G-Mean, which provide a comprehensive measure of performance, particularly in the context of unbalanced data. These metrics make it possible to go beyond the limits of accuracy, which is often insufficient in this context, and underline the relevance of using complex models such as RL for financial risk classification tasks.

Now that the analysis of classification models has been completed, our attention turns to the empirical evaluation of the performance of our proposed Value-at-Risk (VaR) model. In order to obtain an accurate and robust VaR estimate, it is essential to use adequate modeling of the conditional volatility dynamics of financial returns, which often exhibit features such as heteroskedasticity, leptokurtosis, and asymmetry. With this in mind, in addition to the standard GARCH model, we have chosen a GJR-GARCH type conditional volatility structure, which captures the leverage effect, i.e. the tendency of bad news to increase volatility more than good news.

This choice is justified by the asymmetrical nature of financial returns, particularly in equity markets such as the Euro Stoxx 50, where negative shocks have a disproportionate impact on conditional variance. In addition to the dynamic specification of the model, it is imperative to choose an appropriate conditional distribution to model process innovations. Although the normal distribution is a classic choice, it tends to underestimate extreme events due to its thin tails. To overcome this limitation, we explored other fat-tailed distributions and settled on the Student distribution.

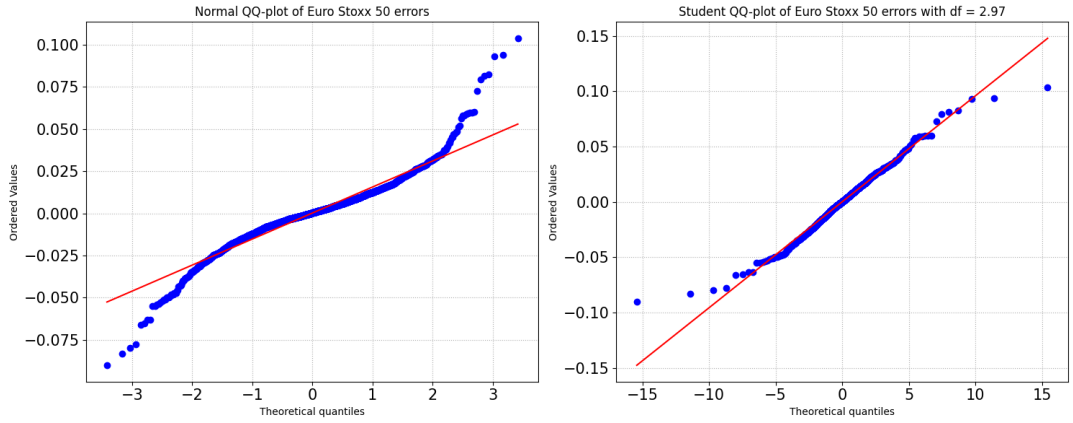

Figure 8: QQ-plot of Euro Stoxx 50 errors distribution

This choice is motivated by the empirical characteristics observed in the distribution of the Euro Stoxx 50 returns, as shown by the statistics presented in table 1, which reveal strong kurtosis and marked asymmetry. These properties are also confirmed by the quantile-quantile plot (QQ plot) illustrated in figure 8, which shows notable deviations from normality, especially in the tails of the distribution. Thus, the adoption of the Student distribution in our GARCH (resp GJR-GARCH) specification not only better captures extreme risks, but also improves the model's fit to empirical data. By combining flexible modeling of conditional volatility with a more realistic distribution of returns, our approach aims to provide more accurate VaR estimates that are better adapted to real market conditions.

The analysis of the Value-at-Risk (VaR) models presented in tables 6, 7, and 8 highlights the superior performance of the Reinforcement Learning (RL)-based model, particularly when coupled with the volatility structures GARCH and GJR-GARCH. In table 6, the statistical indicators show that the RL model has better control over the extremes of the distribution, with lower skewness and kurtosis values than the conventional models, indicating a more symmetrical and less leptokurtic distribution. In the test sample, the $VaR_{RL}^{\text{GARCH}}(\alpha = 5\%)$ model has a skewness of -2.048 and a kurtosis of 8.613, significantly lower than the conventional versions, suggesting a better fit to the empirical characteristics of financial returns.

Model	Version	Min	Median	Mean	Std	Skewness	Kurtosis	Max
$VaR^{\text{GARCH}}(\alpha = 5\%)$	Original	-0.136	-0.013	-0.016	0.012	-5.101	35.265	-0.005
	TCN	-0.129	-0.010	-0.014	0.012	-4.747	31.630	-0.004
	RL	-0.138	-0.010	-0.014	0.011	-4.929	36.258	-0.004
$VaR^{\text{GJR}}(\alpha = 5\%)$	Original	-0.148	-0.013	-0.016	0.012	-5.436	40.562	-0.005
	TCN	-0.141	-0.010	-0.014	0.012	-4.891	35.097	-0.004
	RL	-0.137	-0.011	-0.014	0.012	-5.092	38.121	-0.004
$VaR^{\text{GARCH}}(\alpha = 1\%)$	Original	-0.194	-0.022	-0.027	0.018	-4.481	27.036	-0.011
	TCN	-0.190	-0.017	-0.024	0.018	-4.280	25.984	-0.008
	RL	-0.205	-0.017	-0.023	0.018	-4.402	29.152	-0.008
$VaR^{\text{GJR}}(\alpha = 1\%)$	Original	-0.215	-0.021	-0.027	0.019	-4.772	31.483	-0.010
	TCN	-0.210	-0.017	-0.024	0.019	-4.350	28.127	-0.007
	RL	-0.204	-0.018	-0.023	0.019	-4.534	30.670	-0.007

(a) On validation sample

Model	Version	Min	Median	Mean	Std	Skewness	Kurtosis	Max
$VaR^{\text{GARCH}}(\alpha = 5\%)$	Original	-0.059	-0.015	-0.017	0.005	-2.588	13.231	-0.008
	TCN	-0.071	-0.014	-0.015	0.007	-2.118	9.694	-0.005
	RL	-0.069	-0.013	-0.015	0.006	-2.048	8.613	-0.005
$VaR^{\text{GJR}}(\alpha = 5\%)$	Original	-0.054	-0.015	-0.017	0.006	-2.033	6.564	-0.007
	TCN	-0.065	-0.014	-0.016	0.008	-1.759	5.142	-0.005
	RL	-0.057	-0.013	-0.015	0.007	-1.757	4.732	-0.005
$VaR^{\text{GARCH}}(\alpha = 1\%)$	Original	-0.097	-0.026	-0.028	0.008	-2.485	11.885	-0.014
	TCN	-0.116	-0.024	-0.026	0.011	-2.031	8.645	-0.010
	RL	-0.116	-0.022	-0.025	0.010	-2.058	8.783	-0.010
$VaR^{\text{GJR}}(\alpha = 1\%)$	Original	-0.083	-0.026	-0.028	0.009	-1.997	6.015	-0.013
	TCN	-0.100	-0.023	-0.026	0.013	-1.723	4.754	-0.010
	RL	-0.096	-0.022	-0.025	0.011	-1.773	4.874	-0.010

(b) On testing sample

Table 6: Statistical indicators for VaR models

In addition, the medians and means of the VaR series under LR are more conservative, reflecting a conservative estimate of risk, essential for robust risk management decisions. The results in table 7 (Christoffersen test) (Christoffersen, 1998) confirm the statistical validity of the RL model. Unlike conventional (original) models, which are systematically rejected (p-value $< 5\%$), the RL model is accepted in all configurations, in the validation or test sample, and for confidence levels of 5% and 1%. The Christoffersen test, which verifies the correct calibration of VaR violations, thus validates the ability of the RL model to provide forecasts consistent with observed returns.

Model	Version	Expected violations	Actual violations	Test statistic	Test critical value	Test p-value	Decision
$VaR^{GARCH}(\alpha = 5\%)$	Original	50	73	9.4259	3.8414	0.0368	Reject H_0
	TCN	50	72	8.6521	3.8414	0.0032	Reject H_0
	RL	50	52	0.0075	3.8414	0.9310	Accept H_0
$VaR^{GJR}(\alpha = 5\%)$	Original	50	68	5.8597	3.8414	0.0154	Reject H_0
	TCN	50	72	8.6521	3.8414	0.0032	Reject H_0
	RL	50	53	0.4234	3.8414	0.5002	Accept H_0
$VaR^{GARCH}(\alpha = 1\%)$	Original	10	19	6.3276	3.8414	0.0118	Reject H_0
	TCN	10	25	13.9951	3.8414	0.0002	Reject H_0
	RL	10	12	0.8288	3.8414	0.3856	Accept H_0
$VaR^{GJR}(\alpha = 1\%)$	Original	10	19	6.3276	3.8414	0.0118	Reject H_0
	TCN	10	24	13.9951	3.8414	0.0002	Reject H_0
	RL	10	11	0.0824	3.8414	0.7741	Accept H_0

(a) On validation sample

Model	Version	Expected violations	Actual violations	Test statistic	Test critical value	Test p-value	Decision
$VaR^{GARCH}(\alpha = 5\%)$	Original	50	64	3.5722	3.8414	0.0587	Accept H_0
	TCN	50	47	0.2467	3.8414	0.6193	Accept H_0
	RL	50	52	0.0075	3.8414	0.9310	Accept H_0
$VaR^{GJR}(\alpha = 5\%)$	Original	50	64	3.5722	3.8414	0.0587	Accept H_0
	TCN	50	52	0.0529	3.8414	0.8180	Accept H_0
	RL	50	55	0.4297	3.8414	0.5121	Accept H_0
$VaR^{GARCH}(\alpha = 1\%)$	Original	10	13	0.7828	3.8414	0.3762	Accept H_0
	TCN	10	13	0.7828	3.8414	0.3762	Accept H_0
	RL	10	11	0.0823	3.8414	0.7741	Accept H_0
$VaR^{GJR}(\alpha = 1\%)$	Original	10	12	0.3481	3.8414	0.5551	Accept H_0
	TCN	10	10	0.0006	3.8414	0.9797	Accept H_0
	RL	10	11	0.0824	3.8414	0.7741	Accept H_0

(b) On testing sample

Table 7: Christoffersen test of VaR models

Model	Version	Test statistic	Test critical value	Test p-value	Decision
$VaR^{GARCH}(\alpha = 5\%)$	Original	13.4338	5.9914	0.0012	Reject H_0
	TCN	10.2577	5.9914	0.0059	Reject H_0
	RL	7.6298	5.9914	0.0320	Reject H_0
$VaR^{GJR}(\alpha = 5\%)$	Original	5.9509	5.9914	0.0510	Accept H_0
	TCN	10.2577	5.9914	0.0059	Reject H_0
	RL	5.9593	5.9914	0.0510	Accept H_0
$VaR^{GARCH}(\alpha = 1\%)$	Original	7.0584	5.9914	0.02932	Reject H_0
	TCN	16.0076	5.9914	0.0003	Reject H_0
	RL	4.5624	5.9914	0.1021	Accept H_0
$VaR^{GJR}(\alpha = 1\%)$	Original	0.9907	5.9914	0.6093	Accept H_0
	TCN	15.1671	5.9914	0.0005	Reject H_0
	RL	3.4969	5.9914	0.1740	Accept H_0

(a) On validation sample

Model	Version	Test statistic	Test critical value	Test p-value	Decision
$VaR^{GARCH}(\alpha = 5\%)$	Original	4.5021	5.9914	0.1052	Accept H_0
	TCN	0.2660	5.9914	0.8754	Accept H_0
	RL	1.3806	5.9914	0.5014	Accept H_0
$VaR^{GJR}(\alpha = 5\%)$	Original	3.5735	5.9914	0.1675	Accept H_0
	TCN	0.2643	5.9914	0.8761	Accept H_0
	RL	2.3948	5.9914	0.3019	Accept H_0
$VaR^{GARCH}(\alpha = 1\%)$	Original	1.1229	5.9914	0.5703	Accept H_0
	TCN	1.1229	5.9914	0.5703	Accept H_0
	RL	4.5624	5.9914	0.1021	Accept H_0
$VaR^{GJR}(\alpha = 1\%)$	Original	0.6376	5.9914	0.7270	Accept H_0
	TCN	0.2012	5.9914	0.9042	Accept H_0
	RL	0.3253	5.9914	0.8498	Accept H_0

(b) On testing sample

Table 8: Kupiec test of VaR models

The TCN model also achieves satisfactory results in the test sample, but less systematically than in RL, particularly in terms of stability on the validation sample. This performance is reinforced by the results of table 8 (Kupiec test)(Kupiec et al., 1995), which evaluates the suitability of the number of violations with the expected frequency. Once again, the RL models pass all the tests on the test sample, with p-values well above the critical threshold 5%. This shows that violations are neither too frequent nor too rare and that they do not present a systematic bias.

The RL model is particularly notable in the $VaR^{\text{GARCH}}(\alpha = 1\%)$ and $VaR^{\text{GJR}}(\alpha = 1\%)$ configurations, where it outperforms both the original models and the TCN model. All in all, these results highlight the robustness and accuracy of the RL model, which not only captures market dynamics more realistically through its VaR forecasts, but also meets the rigorous requirements of backtesting tests. The TCN model, while effective in some cases, lags slightly behind in terms of inter-sample stability and overall consistency. RL is therefore the most reliable and efficient model for forecasting extreme risk in volatile financial environments.

4 Discussions

The intrinsic aim of the Value-at-Risk (VaR) model proposed in this study is to correct the recurring biases of traditional models such as GARCH and GJR-GARCH, in particular their tendency to over- or underestimate risk. These models, while robust in their mathematical formulation, have limitations in their ability to adapt dynamically to changing market regimes. These forecasting biases have significant implications for financial institutions, particularly in terms of capital requirements, portfolio management, and regulatory compliance. The use of machine learning, via architectures such as temporal convolutional networks (TCN) and reinforcement learning (RL), aims to dynamically adjust VaR forecasts according to predictive signals from the financial markets, thus improving the model's sensitivity to real variations in risk. More precisely, the VaR regulation mechanism is based on two parameters, b_1 and b_2, which modulate, respectively, the reductions and increases in the initially calculated VaR. In the absence of a universally recognized analytical criterion for their determination, these coefficients were selected by a sensitivity analysis performed on the calibration sample, combined with a rationale for prudent risk management.

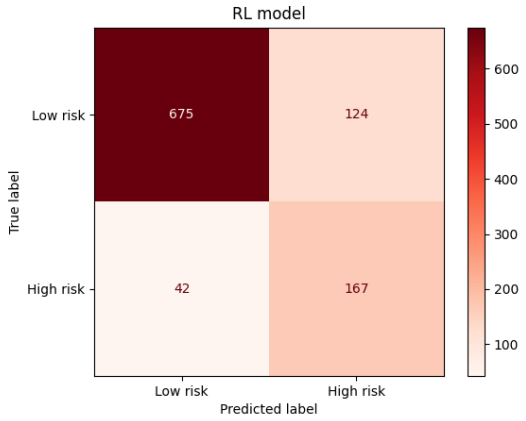

(a) On validation sample

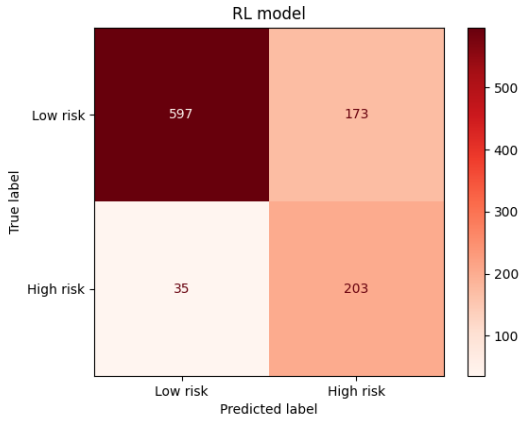

(b) On testing sample

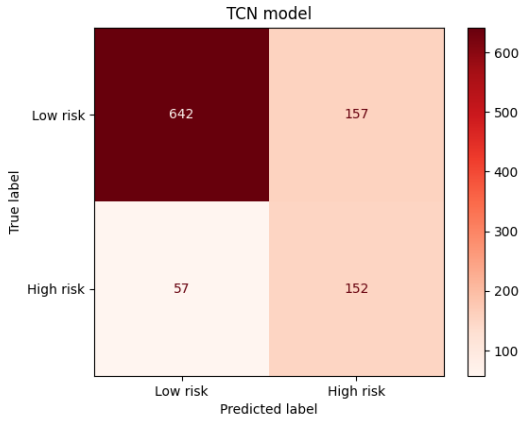

(c) On validation sample

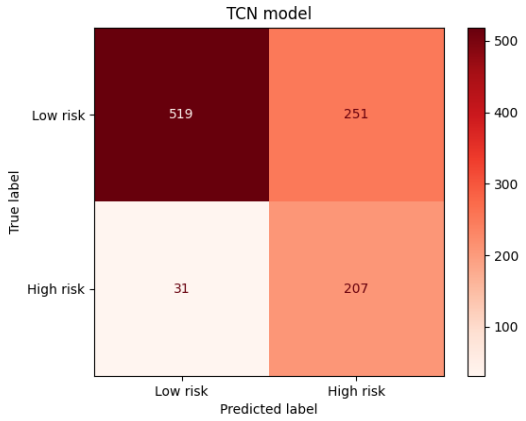

(d) On testing sample

Figure 9: Confusion matrices for RL and TCN models

The chosen values, $b_1 = 0.30$ and $b_2 = 0.20$, reflect a desire to penalize false alarms (risk overestimates) more heavily, while maintaining reinforced hedging in the event of risk underestimation by conventional models. Thus, when the classifier anticipates a 'low risk', the VaR is reduced by 30%, reflecting a unnecessarily tied capital release. In contrast, in the event of high risk, VaR increases by 20%, strengthening prudence in potentially critical periods.

However, the effectiveness of this system depends on the accuracy of the classifier's predictions. The confusion matrices in figure 9 show that the TCN and RL models significantly outperform the other learning models tested. The RL model achieved a high number of good classifications, allowing 675 and 597 justified VaR reductions in the validation and test samples, respectively. At the same time, the TCN model allowed VaR to increase 167 and 203 times, helping to avoid potential breaches of the VaR threshold. These dynamic adjustments result in a better allocation of economic capital, reducing capital requirements without compromising the robustness of risk hedging.

Although some prediction errors remain, notably with the TCN model, which shows a slight increase in the number of VaR violations, these errors have not led to any major failures in risk hedging, as attested by the satisfactory results of backtesting tests (Christoffersen and Kupiec tests). This finding justifies the exclusion of the other machine learning models, which perform less well in classification (see Figures A1 and A2), in the rest of the analysis. Thus, the integration of intelligent classification modules into the VaR calculation process not only makes it possible to refine risk estimates, but above all, to flexibly adapt capital requirements to market conditions.

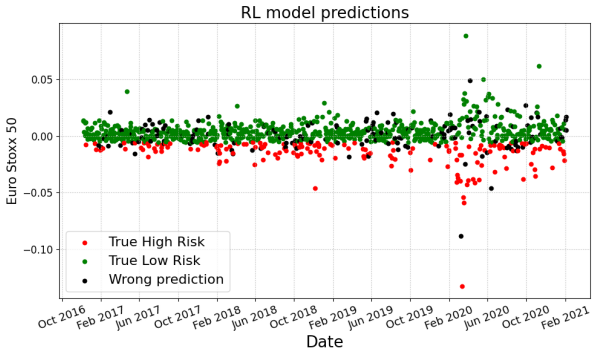

(a) On validation sample

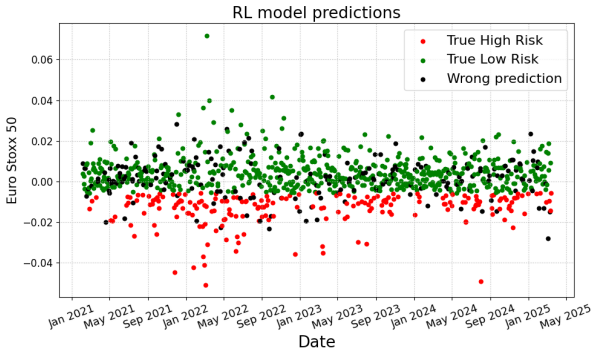

(b) On testing sample

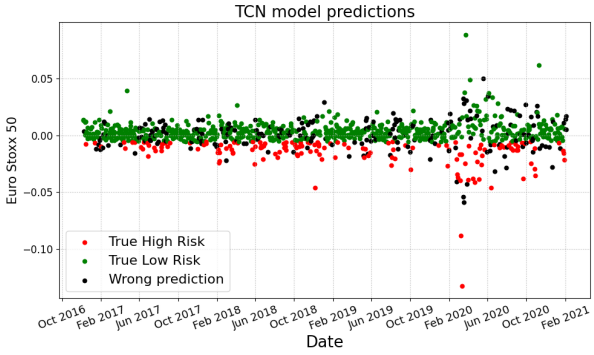

(c) On validation sample

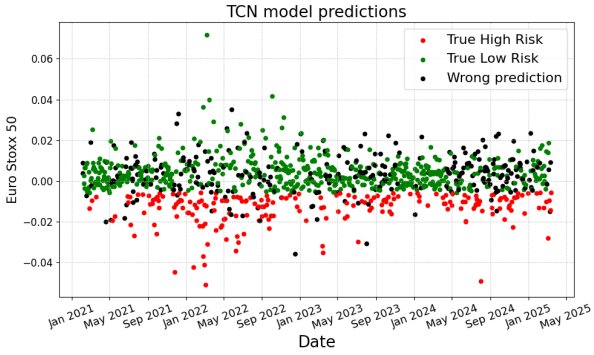

(d) On testing sample

Figure 10: Prediction of risk levels

The proposed model, based on the robust predictions of the TCN and RL classifiers, demonstrates an ability to reconcile statistical rigor and economic efficiency, making it a significant advance in the field of dynamic financial risk management.

The validation and test samples cover the periods from July 7, 2016 to February 3, 2021 and February 4, 2021 to March 13, 2025 respectively, each with 1008 observations corresponding to four years of trading days. These two subperiods, although distinct, share a common feature: high instability in financial markets linked to major exogenous shocks.

The first sample comes at a time of extreme uncertainty marked by the Brexit referendum and, above all, the global health crisis linked to COVID-19. These events profoundly disrupted market dynamics, introducing sudden jumps in volatility, trend breaks, and an increased frequency of systemic shocks. In such an environment, the predictive performance of traditional econometric models, such as GARCH or GJR-GARCH, is often limited by their rigid structure and dependence on stationarity assumptions.

The second sample, although in a post-COVID recovery phase, was nonetheless marked by new sources of instability. Global inflationary pressures, prolonged supply chain disruptions, and Russia's invasion of Ukraine were all major exogenous shocks that increased uncertainty in European markets. These events generated persistent volatility, often marked by sudden alternations between calm phases and episodes of extreme turbulence.

It is precisely in this context that deep learning models such as the Temporal Convolutional Network (TCN) and the Deep Double Q-Learning Network (DDQN), which is our RL model, show their full potential. TCN, with its ability to capture long-term dependencies via dilated causal convolutions, excels at modeling complex, nonlinear temporal structures. This architecture enables a hierarchical representation of financial signals, offering a better adaptation to the fluctuating volatility regimes characteristic of crisis markets (see Pokou et al., 2024b).

By effectively capturing latent patterns, TCN offers more robust Value-at-Risk (VaR) prediction, reducing under- or overestimation errors. In this context, the adaptive structure of DDQN is particularly relevant. Unlike purely statistical models, DDQN is based on active learning through interaction with the financial environment. By defining a reward function that incorporates forecast errors and VaR violations, the model dynamically adjusts risk levels, thus anticipating market reversals more effectively. Its ability to dissociate evaluation and target networks also stabilizes learning and avoids overfitting, significantly improving the robustness of the decisions made.

The ability of these models to integrate temporal heterogeneity and risk asymmetry gives them a decisive edge in forecasting extreme measures such as VaR. Their structural flexibility, their ability to capture alternating volatility regimes, and their adaptive learning capacity make them the tools of choice for risk management in ever-changing financial environments, as shown in figure 10.

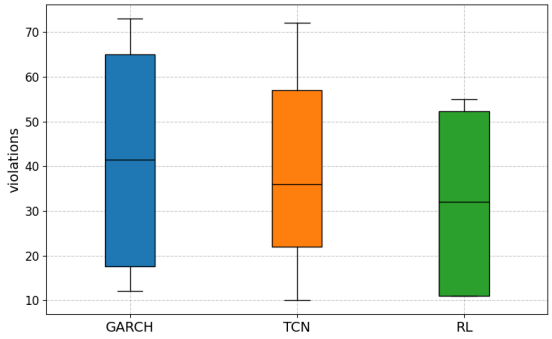

Figure 11: Boxplots of VaR violation

Sample	Model	GARCH	TCN	RL
validation	GARCH 95%	73	72	52
	GJR 95%	68	72	53
	GARCH 99%	19	25	12
	GJR 99%	13	13	11
testing	GARCH 95%	64	47	52
	GJR 95%	64	52	55
	GARCH 99%	13	13	11
	GJR 99%	12	10	11

Table 9: VaR violation

The empirical results of the backtesting, presented in Tables 7 and 8, confirm these strengths: The TCN and DDQN models almost systematically meet the specified confidence thresholds (95% and 99%), while satisfying the Kupiec (unconditional coverage) and Christoffersen (independence of violations) tests. These results illustrate the superiority of machine learning-based approaches, particularly in periods of structurally unstable volatility.

To assess the robustness of the different VaR forecasting models, table 4 summarizes the number of violations observed for all the approaches tested, whether traditional models (GARCH, GJR-GARCH) or machine learning methods (notably TCN and RL), taking into account both the two volatility structures considered and the usual risk thresholds (1% and 5%). This table highlights the differential performance of the models in terms of hedging accuracy, in particular their ability to minimize occurrences of theoretical VaR overshoot. These empirical results are visually confirmed by the violation distributions shown as boxplots in figure 4. However, to go beyond a simple descriptive analysis and guarantee the statistical validity of the observed deviations, a nonparametric Wilcoxon test was applied. The results, presented in table 10, confirm that the RL model shows a significantly lower average number of violations than all other models, at a significance level of 5%.

Test hypotheses	Test indicators	TCN vs GARCH	RL vs GARCH	TCN vs RL
$H_0 : \mu_1 = \mu_2$ vs $H_1 : \mu_1 < \mu_2$	Test statistic	12	0.0	8
	P-value	0.3997	0.0039	0.0976

Table 10: Equality test for VaR violation means

With a p-value of 0.0039, we have strong statistical evidence to conclude that the reinforcement learning (RL) model generates significantly fewer Value-at-Risk (VaR) violations than the GARCH model, under equivalent conditions of volatility and risk thresholds. This result indicates a better performance of the RL model in terms of extreme risk management, which can be interpreted as a greater ability to anticipate and limit exceptional losses. Compared to the TCN (Temporal Convolutional Network) model, the RL model also tends to produce a lower number of violations, but the difference does not reach the conventional statistical significance threshold of 5%.

α	Ind stat	GARCH		GJR-GARCH	
		TCN	RL	TCN	RL
5%	statistic	243568	228198	241408	235833
	p-value	0.1236	0.0136	0.08212	0.02308
1%	statistic	252784	238663	241376	236536
	p-value	0.4362	0.04572	0.08159	0.0436

(a) On validation sample

α	Ind stat	GARCH		GJR-GARCH	
		TCN	RL	TCN	RL
5%	statistic	234618	226652	220530	235833
	p-value	0.01678	0.0014	0.0001	0.02308
1%	statistic	237250	236431	238642	238250
	p-value	0.03284	0.02685	0.0455	0.04159

(b) On testing sample

Table 11: Mann-Whitney test between distributions of $\text{VaR}_{t+1}(\alpha)$ and $\text{VaR}_{ML}(\alpha)$

From the point of view of efficient regulatory capital management, it is essential that Value-at-Risk (VaR) models are not only accurate in terms of covering extreme losses but also conservative without being excessively penalizing. In particular, this means that, where market conditions allow, proposed models should produce less stringent VaR estimates while maintaining an acceptable frequency of violation.

In other words, a high-performance model is one that reduces capital requirements while respecting regulatory risk thresholds. In order to assess the ability of machine learning models to meet this objective, we compared the distribution of VaR values generated by the TCN and RL models to those derived from traditional conditional volatility-based models, such as GARCH and GJR-GARCH. More specifically, Figures 12 and 13 superimpose the empirical distributions of the $\text{VaR}_{t+1}(\alpha)$ values derived from a GJR-GARCH model with those of the values predicted, respectively, by the TCN and RL models, for the risk thresholds $\alpha = 5\%$ and $\alpha = 1\%$.

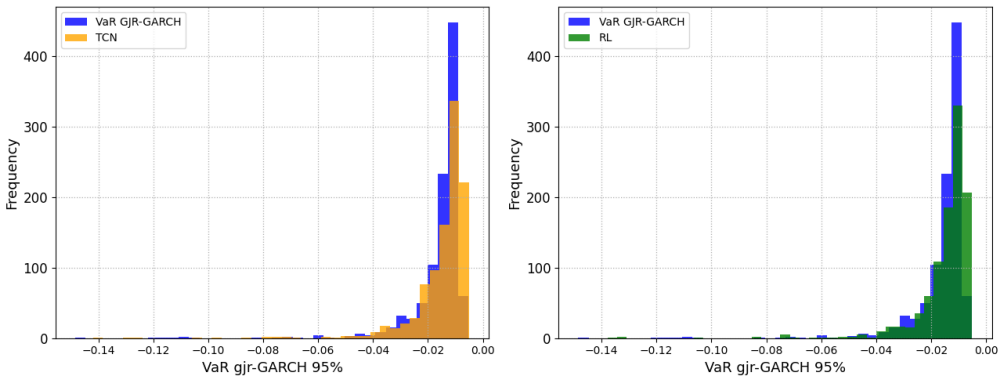

Figure 12: Comparison of VaR distributions with a GJR-GARCH volatility process on the validation sample

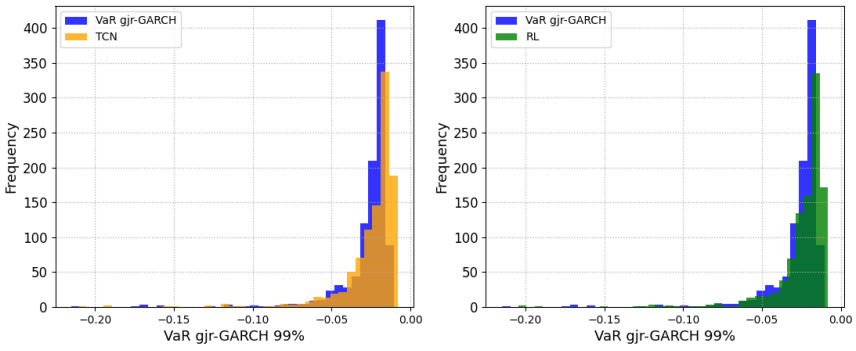

Figure 13: Comparison of VaR distributions with a GJR-GARCH volatility process on the testing sample

A visual inspection of these distributions shows that, in the majority of cases, the distributions resulting from machine learning models are shifted to the right, i.e. their values are less negative in comparison with traditional models. This shift suggests a potential reduction in the capital required to cover extreme losses. To statistically confirm this observation, we use the nonparametric Mann-Whitney test (Mann and Whitney, 1947), which tests the hypothesis that the median of the VaR distribution of machine learning models is higher than that from the GARCH or GJR-GARCH models.

The choice of the median, rather than the mean, is justified by its robustness to extreme values, particularly frequent in the left tail of financial return distributions. In our case, given that all VaR values are negative, a less negative median (i.e. higher in absolute value) implies a lower capital allocation, provided hedging remains sufficient. The test results, presented in table 11, confirm that the medians of the $\text{VaR}_{RL}(\alpha)$ distributions are statistically superior to those of the GARCH-type models, for both samples (validation and test), regardless of the risk threshold (1% or 5%) and the volatility specification used.

In contrast, the results for the TCN model show that its performance is more nuanced. In the validation sample, only one configuration (5% GARCH) leads to a significant difference in the median. However, in the test sample, the differences are significant at all thresholds and for both types of volatility model, but with a smaller magnitude than that observed for the RL. These results suggest that not only are deep learning models in particular the reinforcement model (RL) able to better anticipate VaR violations, but they also do so in a more capital-efficient way. This reinforces their relevance for dynamic risk management, where adaptability to the market environment is crucial.

The financial crisis of 2007-2009 highlighted the many weaknesses in the risk management models used by financial institutions, particularly those based on Value-at-Risk (VaR), which had proved insufficient to anticipate or absorb extreme events. In response, the Basel Committee on Banking Supervision undertook a series of major reforms (Supervision, 2011, 2012; on Banking Supervision, 2017), known as Basel III, one of the most notable of which was the gradual replacement of VaR by a new, more conservative and robust risk measure. Expected Shortfall (ES). Unlike VaR, which evaluates the maximum potential loss at a certain confidence level without providing information on losses beyond this threshold, Expected Shortfall measures the conditional average loss in the event of VaR being exceeded. Mathematically, it is expressed as follows:

$$ES_{t+1}(\alpha) = \mathbb{E}[r_{t+1} \mid r_{t+1} < \text{VaR}_{t+1}(\alpha)]$$

In other words, the expected shortfall is directly related to VaR insofar as it is based on knowledge of the latter. Thus, building a robust VaR model remains an essential prerequisite to estimating the expected shortfall, especially when modeling distribution tails in a context of strong asymmetries and conditional volatility. In this sense, even if VaR is no longer a central regulatory measure, it remains a fundamental component of the risk calculation chain. In this context, our approach is fully in line with current risk management concerns.

Indeed, we propose VaR estimation using deep learning models, notably the Temporal Convolutional Network (TCN) and Reinforcement Learning (RL) architectures, capable of better capturing the complex temporal dynamics of financial series. These models differ from traditional parametric approaches in their ability to incorporate a large historical memory, to learn about nonlinear relationships between variables, and to adapt to changing market regimes.

The use of TCN, for example, enables efficient handling of long-time dependencies while retaining a convolutional structure that facilitates parallelization and speeds up training compared to conventional RNNs. As for the RL model, it introduces a dynamic optimization dimension, by learning a policy that maximizes a reward associated with the correct VaR estimate, which is particularly relevant in an active risk management framework.

However, these models also have certain limitations. Their implementation requires a relatively long calibration phase, high sensitivity to hyperparameters, and advanced algorithmic expertise. In addition, their interpretability may be less than that of traditional models, which can be a hindrance in regulatory contexts that require a clear justification for decisions. These considerations, while essential from an operational perspective, will not be addressed in depth in the present work, which focuses on the empirical evaluation of predictive performance. Ultimately, by proposing an improved model of VaR, this work provides a solid basis for estimating Expected Shortfall, while contributing to contemporary debates on the integration of artificial intelligence techniques into risk management systems. The relevance of VaR therefore remains intact, not only as a standalone tool but also as a methodological foundation for more advanced measures in line with current regulatory standards.

5 Conclusion

This paper introduced a novel methodology for Value-at-Risk (VaR) estimation designed to reduce both the number of risk violations and the capital reserves required for market risk coverage. The core innovation lies in the dynamic adjustment of the VaR level based on a predictive classification of return risk, allowing for more conservative thresholds during turbulent periods and less stringent capital constraints during calmer market regimes. To achieve this, we reformulated the problem of return forecasting into an imbalanced classification task a well-known challenge in financial time series modeling due to the inherent asymmetry and rarity of extreme events.

Addressing this complexity, we leveraged the Double Deep Q-Network (DDQN), a reinforcement learning algorithm grounded in deep learning architectures. Unlike traditional classifiers, DDQN learns an optimal policy for decision making under uncertainty, enabling it to handle temporal dependencies and adapt its classification strategy based on past prediction errors and changing market conditions. Empirical results show that the VaR forecasts produced by our DDQN-based approach consistently outperform those of benchmark models in terms of backtest performance and capital efficiency. Furthermore, the ability of the model to anticipate changes in market risk by learning from its environment through reward-based feedback confers a strategic advantage in dynamic risk management.

Our contribution is twofold. First, we advance the econometric literature on risk measures by proposing an AI-enhanced VaR model capable of adaptive behavior in volatile financial environments. Second, we contribute to the broader field of data science by demonstrating the effectiveness of reinforcement learning, and specifically DDQN, in solving imbalanced classification problems in the context of financial time series.

Future work may explore the integration of alternative reinforcement learning paradigms and further refine model calibration techniques to enhance interpretability and computational efficiency, an important consideration, given the model's parametric complexity and training time, which we acknowledge as a limitation not addressed in the present study.

Compliance with Ethical Standards

Declaration of Competing Interest

All authors declare that they have no conflicts of interest.

Ethical approval:

This article does not contain any studies with human participants or animals performed by any of the authors.

References

H. Alostad and H. Davulcu. Directional prediction of stock prices using breaking news on twitter. In *Web Intelligence*, volume 15, pages 1–17. IOS Press, 2017.

E. K. Ampomah, Z. Qin, and G. Nyame. Evaluation of tree-based ensemble machine learning models in predicting stock price direction of movement. *Information*, 11(6):332, 2020.

R. Barandela, R. M. Valdovinos, J. S. Sánchez, and F. J. Ferri. The imbalanced training sample problem: Under or over sampling? In *Structural, Syntactic, and Statistical Pattern Recognition: Joint IAPR International Workshops, SSPR 2004 and SPR 2004, Lisbon, Portugal, August 18-20, 2004. Proceedings*, pages 806–814. Springer, 2004.

D. Barrera, S. Crépey, E. Gobet, H.-D. Nguyen, and B. Saadeddine. Learning value-at-risk and expected shortfall. 2022.

J. Becker and C. Leschinski. Directional predictability of daily stock returns. Technical report, Hannover Economic Papers (HEP), 2018.

T. Bollerslev. Generalized autoregressive conditional heteroskedasticity. *Journal of econometrics*, 31 (3):307–327, 1986.

V. Chandrasekara, C. Tilakaratne, and M. Mammadov. An improved probabilistic neural network model for directional prediction of a stock market index. *Applied Sciences*, 9(24):5334, 2019.

N. V. Chawla, K. W. Bowyer, L. O. Hall, and W. P. Kegelmeyer. Smote: synthetic minority over-sampling technique. *Journal of artificial intelligence research*, 16:321–357, 2002.

P. F. Christoffersen. Evaluating interval forecasts. *International economic review*, pages 841–862, 1998.

J. Chung and Y. Hong. Model-free evaluation of directional predictability in foreign exchange markets. *Journal of Applied Econometrics*, 22(5):855–889, 2007.

W. R. Clements, B. Van Delft, B.-M. Robaglia, R. B. Slaoui, and S. Toth. Estimating risk and uncertainty in deep reinforcement learning. *arXiv preprint arXiv:1905.09638*, 2019.

Y. Deng, F. Bao, Y. Kong, Z. Ren, and Q. Dai. Deep direct reinforcement learning for financial signal representation and trading. *IEEE transactions on neural networks and learning systems*, 28 (3):653–664, 2016.

A. K. Dixit. *Optimization in economic theory*. Oxford University Press, USA, 1990.

S. Dreiseitl and L. Ohno-Machado. Logistic regression and artificial neural network classification models: a methodology review. *Journal of biomedical informatics*, 35(5-6):352–359, 2002.

T. Elhassan and M. Aljurf. Classification of imbalance data using tomek link (t-link) combined with random under-sampling (rus) as a data reduction method. *Global J Technol Optim S*, 1:2016, 2016.

E. F. Fama. Efficient capital markets: A review of theory and empirical work. *The journal of Finance*, 25(2):383–417, 1970.

T. Fawcett and F. Provost. Adaptive fraud detection. *Data mining and knowledge discovery*, 1(3): 291–316, 1997.

W. R. Gilks, S. Richardson, and D. Spiegelhalter. *Markov chain Monte Carlo in practice*. CRC press, 1995.

L. R. Glosten, R. Jagannathan, and D. E. Runkle. On the relation between the expected value and the volatility of the nominal excess return on stocks. *The journal of finance*, 48(5):1779–1801, 1993.

I. Goodfellow, Y. Bengio, A. Courville, and Y. Bengio. *Deep learning*, volume 1. MIT press Cambridge, 2016.

S. Gu, E. Holly, T. Lillicrap, and S. Levine. Deep reinforcement learning for robotic manipulation with asynchronous off-policy updates. In *2017 IEEE international conference on robotics and automation (ICRA)*, pages 3389–3396. IEEE, 2017.

H. Han, W.-Y. Wang, and B.-H. Mao. Borderline-smote: a new over-sampling method in imbalanced data sets learning. In *International conference on intelligent computing*, pages 878–887. Springer, 2005.

B. Jang, M. Kim, G. Harerimana, and J. W. Kim. Q-learning algorithms: A comprehensive classification and applications. *IEEE access*, 7:133653–133667, 2019.

A. Kanas. Neural network linear forecasts for stock returns. *International Journal of Finance & Economics*, 6(3):245–254, 2001.

S. Kotsiantis, D. Kanellopoulos, P. Pintelas, et al. Handling imbalanced datasets: A review. *GESTS international transactions on computer science and engineering*, 30(1):25–36, 2006.

P. H. Kupiec et al. *Techniques for verifying the accuracy of risk measurement models*, volume 95. Division of Research and Statistics, Division of Monetary Affairs, Federal . . . , 1995.

M. B. Kursa and W. R. Rudnicki. Feature selection with the boruta package. *Journal of statistical software*, 36:1–13, 2010.

M. B. Kursa, A. Jankowski, and W. R. Rudnicki. Boruta–a system for feature selection. *Fundamenta Informaticae*, 101(4):271–285, 2010.

C. Lea, R. Vidal, A. Reiter, and G. D. Hager. Temporal convolutional networks: A unified approach to action segmentation. In *Computer Vision–ECCV 2016 Workshops: Amsterdam, The Netherlands, October 8-10 and 15-16, 2016, Proceedings, Part III 14*, pages 47–54. Springer, 2016.

O. Linton and Y.-J. Whang. The quantilogram: With an application to evaluating directional predictability. *Journal of Econometrics*, 141(1):250–282, 2007.

X.-Y. Liu, H. Yang, Q. Chen, R. Zhang, L. Yang, B. Xiao, and C. D. Wang. Finrl: A deep reinforcement learning library for automated stock trading in quantitative finance. *arXiv preprint arXiv:2011.09607*, 2020.

H. B. Mann and D. R. Whitney. On a test of whether one of two random variables is stochastically larger than the other. *The annals of mathematical statistics*, pages 50–60, 1947.

H. Mao, M. Alizadeh, I. Menache, and S. Kandula. Resource management with deep reinforcement learning. In *Proceedings of the 15th ACM workshop on hot topics in networks*, pages 50–56, 2016.

H. Markowitz. Portfolio selection. *Journal of Finance*, 1952.

H. M. Markowitz. Portfolio selection: E cient diversification of investments. *Cowles Foundation Monograph*, 16, 1959.

V. Mnih, K. Kavukcuoglu, D. Silver, A. Graves, I. Antonoglou, D. Wierstra, and M. Riedmiller. Playing atari with deep reinforcement learning. *arXiv preprint arXiv:1312.5602*, 2013.

T. Morimura, M. Sugiyama, H. Kashima, H. Hachiya, and T. Tanaka. Parametric return density estimation for reinforcement learning. *arXiv preprint arXiv:1203.3497*, 2012.

F. Murtagh. Multilayer perceptrons for classification and regression. *Neurocomputing*, 2(5-6):183–197, 1991.

L. Nevasalmi. Forecasting multinomial stock returns using machine learning methods. *The Journal of Finance and Data Science*, 6:86–106, 2020.

H. Nyberg. Forecasting the direction of the us stock market with dynamic binary probit models. *International Journal of Forecasting*, 27(2):561–578, 2011.

C. Oh and O. Sheng. Investigating predictive power of stock micro blog sentiment in forecasting future stock price directional movement. 2011.

B. C. on Banking Supervision. Basel iii: Finalising post-crisis reforms. *Bank for International Settlements*, 2017.

R. M. Pereira, Y. M. Costa, and C. N. Silla Jr. Mltl: A multi-label approach for the tomek link undersampling algorithm. *Neurocomputing*, 383:95–105, 2020.

F. Pokou, J. S. Kamdem, and F. Benhmad. Deep reinforcement learning for an empirical approach to value-at-risk. 2024a.

F. Pokou, J. Sadefo Kamdem, and F. Benhmad. Hybridization of arima with learning models for forecasting of stock market time series. *Computational Economics*, 63(4):1349–1399, 2024b.

F. V. M. Pokou. *Une contribution sur l'allocation ou la prévision d'actifs d'un portefeuille.* PhD thesis, Université de Montpellier, 2022.

M. L. Puterman. *Markov decision processes: discrete stochastic dynamic programming.* John Wiley & Sons, 2014.

F. Rosenblatt. The perceptron: a probabilistic model for information storage and organization in the brain. *Psychological review*, 65(6):386, 1958.

M. A. I. Sunny, M. M. S. Maswood, and A. G. Alharbi. Deep learning-based stock price prediction using lstm and bi-directional lstm model. In *2020 2nd novel intelligent and leading emerging sciences conference (NILES)*, pages 87–92. IEEE, 2020.

B. Supervision. Basel committee on banking supervision. *Principles for Sound Liquidity Risk Management and Supervision (September 2008)*, 2011.

B. Supervision. Basel committee on banking supervision. 2012.

R. Sutton and A. Barto. Reinforcement learning: An introduction. *IEEE Transactions on Neural Networks*, 9(5):1054–1054, 1998.

R. S. Sutton. Learning to predict by the methods of temporal differences. *Machine learning*, 3:9–44, 1988.

C. Szepesvári. Value prediction problems. In *Algorithms for Reinforcement Learning*, pages 11–36. Springer, 2010.

Y. Tang, Y.-Q. Zhang, N. V. Chawla, and S. Krasser. Svms modeling for highly imbalanced classification. *IEEE Transactions on Systems, Man, and Cybernetics, Part B (Cybernetics)*, 39(1):281–288, 2008.

A. Tealab. Time series forecasting using artificial neural networks methodologies: A systematic review. *Future Computing and Informatics Journal*, 3(2):334–340, 2018.

H. Van Hasselt, A. Guez, and D. Silver. Deep reinforcement learning with double q-learning. In *Proceedings of the AAAI conference on artificial intelligence*, volume 30, 2016.

V. Vapnik. *The nature of statistical learning theory.* Springer science & business media, 1999.

C. J. C. H. Watkins. Learning from delayed rewards. 1989.

C. C. White III and D. J. White. Markov decision processes. *European Journal of Operational Research*, 39(1):1–16, 1989.

H. Yang, X.-Y. Liu, S. Zhong, and A. Walid. Deep reinforcement learning for automated stock trading: An ensemble strategy. In *Proceedings of the first ACM international conference on AI in finance*, pages 1–8, 2020.

C. Ying, X. Zhou, H. Su, D. Yan, N. Chen, and J. Zhu. Towards safe reinforcement learning via constraining conditional value-at-risk. *arXiv preprint arXiv:2206.04436*, 2022.

C. Yu, J. Liu, S. Nemati, and G. Yin. Reinforcement learning in healthcare: A survey. *ACM Computing Surveys (CSUR)*, 55(1):1–36, 2021.

M. Zeng, B. Zou, F. Wei, X. Liu, and L. Wang. Effective prediction of three common diseases by combining smote with tomek links technique for imbalanced medical data. In *2016 IEEE International Conference of Online Analysis and Computing Science (ICOACS)*, pages 225–228. IEEE, 2016.

G. P. Zhang. Time series forecasting using a hybrid arima and neural network model. *Neurocomputing*, 50:159–175, 2003.

H. Zhang and M. Li. Rwo-sampling: A random walk over-sampling approach to imbalanced data classification. *Information Fusion*, 20:99–116, 2014.

Z. Zhang, S. Zohren, and R. Stephen. Deep reinforcement learning for trading. *The Journal of Financial Data Science*, 2020.

X. Zhao, L. Zhang, L. Xia, Z. Ding, D. Yin, and J. Tang. Deep reinforcement learning for list-wise recommendations. *arXiv preprint arXiv:1801.00209*, 2017.

A Confusion matrices

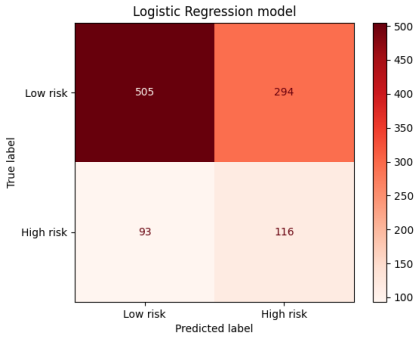

(a) On validation sample

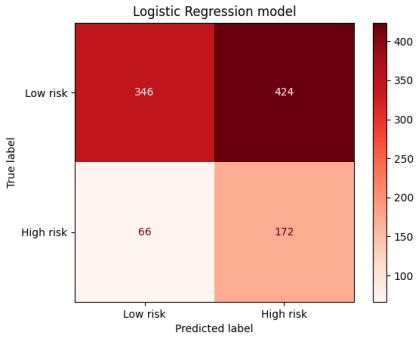

(b) On testing sample

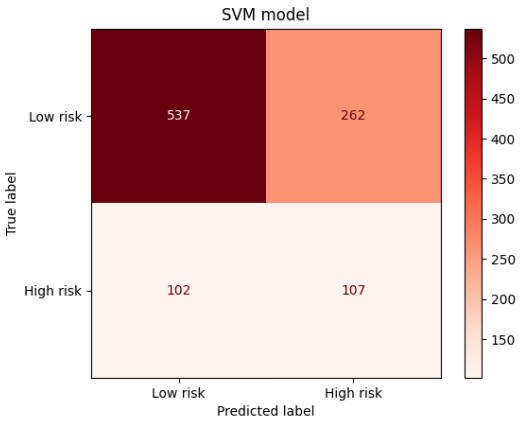

(c) On validation sample

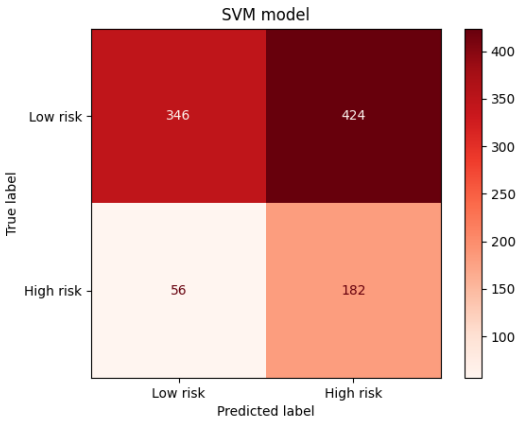

(d) On testing sample

Figure A1: Confusion matrices for learning models

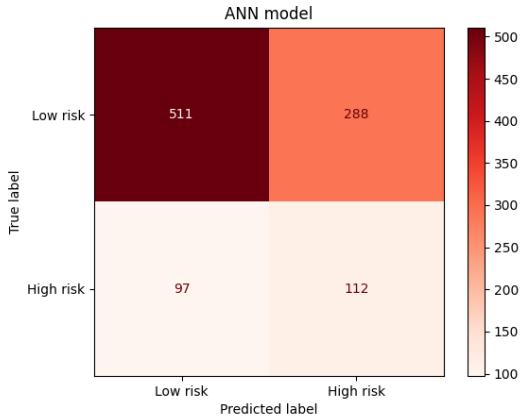

(a) On validation sample

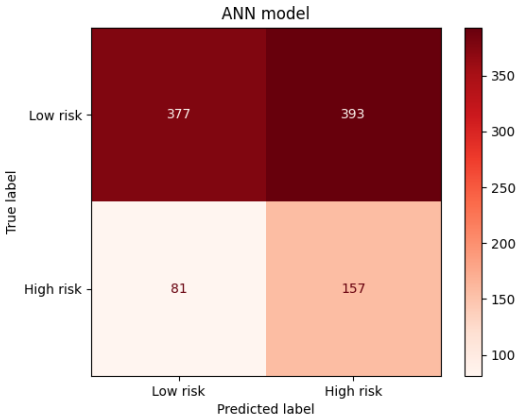

(b) On testing sample

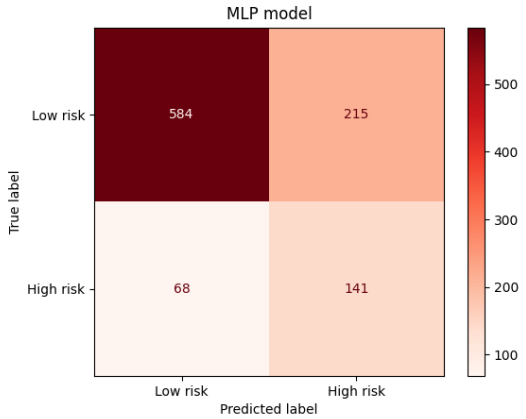

(c) On validation sample

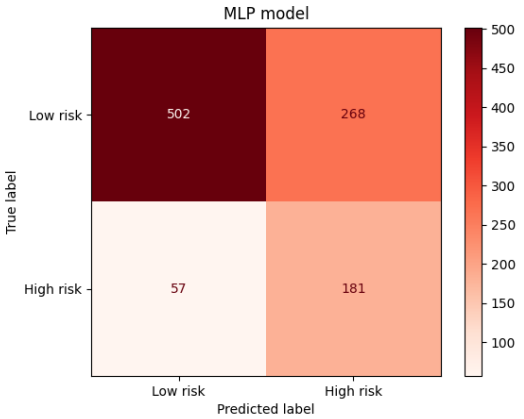

(d) On testing sample

Figure A2: Confusion matrices for learning models

B Selected features

nº	Asset	ID	Informations
1	AEX	^AEX	Index
2	CAC 40	^FCHI	Index
3	DAX	^GDAXI	Index
4	Euro Stoxx 50	^STOXX50E	Index
5	Brent Crude Oil Last Day	BZ=F	Commodity
6	EURO/USD	EURUSD=X	Currency
7	EURO/GBP	EURGBP=X	Currency
8	SPDR EURO STOXX 50 ETF	FEZ	ETF
9	Bollinger Bands	BB upper & BB lower	Technical trading indicator
10	Relative Strength Index	RSI 14	Technical trading indicator
11	Standard Moving Average	SMA 5 & SMA 15	Technical trading indicator
12	Exponentially Weighted Moving Average	EMA 5 & EMA 15	Technical trading indicator
13	Forecasting returns using GARCH model	^STOXX50E mu GARCH	Econometric indicators
14	Forecasting volatility using GARCH model	^STOXX50E sig GARCH	Econometric indicators
15	Forecasting volatility using GJR6GARCH model	^STOXX50E sig gjr-GARCH	Econometric indicators
16	Forecasting VaR using GARCH model	^STOXX50E VaR GARCH	Econometric indicators
17	Forecasting VaR using GJR-GARCH model	^STOXX50E VaR gjr-GARCH	Econometric indicators
18	SMA strategy trading positions	Signal 1	Technical trading indicator
19	EMA strategy trading positions	Signal 2	Technical trading indicator
20	BB strategy trading positions	Signal 3	Technical trading indicator
21	Forecasting risk level of returns with ARIMA model	ARIMA indicator	Class prediction

Table B1: Selected features